

# **Direct conversion of chemical energy to mechanical work using a phosphate charged protein**

Ying Shen

Thesis submitted to the faculty of the  
Virginia Polytechnic Institute and State University  
in partial fulfillment of the requirements for the degree of

Master of Science  
In  
Biological Systems Engineering

Justin R. Barone, Chair  
Ryan Senger, Committee Member  
Joseph Warren Freeman, Committee Member

April 9, 2010  
Blacksburg, VA

Keywords: casein, protein gel, dephosphorylation, re-phosphorylation, energy

# **Direct conversion of chemical energy to mechanical work using a phosphate charged protein**

Ying Shen

## **ABSTRACT**

Nature is able to convert chemical energy into mechanical work under modest conditions, i.e., physiological pH and ambient temperature and pressure. One of the most interesting systems is muscle modeled as the “sliding filament” system. The sliding filament system is a combination of a thin actin filament and a thick myosin filament that slide over one another by breaking the "energy-rich" pyrophosphate bond of ATP. The energy from ATP hydrolysis is used for mechanical motion and the energy lost during this process is used to heat our body. In biology, the sliding filament system is taken as a fairly effective model. For engineering systems, the energy lost to heat needs to be reduced to build an efficient energy converter.

In our research, we use a phosphate charged protein, casein, and react it with divinyl sulfone (DVS) through a Michael addition reaction to produce a cross-linked gel. The protein gel could be dephosphorylated at standard conditions using bovine phosphatase (bp) and re-phosphorylated using casein kinase. When attached to the protein, the negatively charged phosphate groups cause the gel to expand from repulsion. When removed, the protein contracts. Therefore, work is realized without sliding friction, which is the origin of the large energy loss in muscle. FT-IR spectroscopy allows us to follow the two biochemical reactions. We also show a thermodynamic analysis of the work and offer an estimation of the most basic term.

## ACKNOWLEDGEMENTS

I would like to take this chance to show my appreciation for my advisor Dr. Justin Barone. In the past two years, he has been patient enough to lead me into the realm of research and teach me the basic exploration principles. Your attitude toward work and enthusiasm for your engagement always motivates me.

I also would like to thank my senior lab mate Naresh Budhavaram who gave me lots of earnest help and care. The genuine friendship we developed will warm me for a whole life.

Additionally, I would like to thank Dr. Ryan Senger and Dr. Joseph Warren Freeman for helpful advice and guidance on my thesis.

Finally, I will like to appreciate my boyfriend Junqi Gao's sincere support in every aspects and send my mother and father everlasting feelings of gratefulness and thankfulness. "To do your job with soul", which you taught me, always urges me on the way. Your love drives me to be here today.

# CONTENTS

<b>ACKNOWLEDGEMENTS</b> .....	iii
<b>CONTENTS</b> .....	iv
<b>CHAPTER 1</b> .....	1
1.1 References:.....	4
<b>CHAPTER 2</b> .....	5
2.1 Muscle protein filament.....	5
2.1.1 Structure of sarcomere .....	5
2.1.2 Myosin filament.....	7
2.1.3 Actin filament .....	7
2.1.4 Molecular mechanism of muscle movement .....	8
2.2 Ionic polymer gel .....	10
2.3 Synthesis of protein machine .....	11
2.3.1 Design principle of protein machine.....	11
2.3.2 Casein.....	12
2.3.3 Michael addition .....	12
2.3.4 Synthesis of protein machine .....	13
2.4 References:.....	15
<b>CHAPTER 3</b> .....	18
3.1 Introduction.....	18
3.2 Materials and methods .....	19
3.2.1 Materials .....	19
3.2.2 Dephosphorylation activity of bovine phosphatase and potato acid phosphatase on 4-np.....	19
3.2.3 Dephosphorylation of uncross-linked casein and casein kinase substrate with bovine phosphatase (bp) .....	19
3.2.4 Cross-linking casein with DVS.....	20
3.2.5 Measurement of contraction cycle .....	20
3.3 Results.....	20
3.3.1 UV-Visible results of dephosphorylation activity of bovine phosphatase and potato acid phosphatase.....	20
3.3.2 Protein machine and its characterization .....	22
3.4 Discussion.....	28
3.5 Conclusions.....	31
3.6 References:.....	32
<b>CHAPTER 4</b> .....	33
4.1 Abstract.....	33
4.2 Introduction.....	33
4.3 Materials and methods .....	34
4.3.1 Materials .....	34
4.3.2 Preparation of protein machine.....	34
4.3.3 Preparation of re-phosphorylated casein rubber .....	34
4.3.4 Fourier transform-infrared (FT-IR) spectroscopy.....	36
4.4 Results.....	37
4.4.1 Phosphorylation of casein kinase substrate.....	37

4.4.2	Demonstration of one full protein machine cycle.....	37
4.4.3	Fourier transform-infrared (FT-IR) spectroscopy.....	40
4.5	Thermodynamic Analysis of the Protein Machine .....	46
4.6	Conclusion .....	50
4.7	References:.....	51
CHAPTER 5	.....	53

## List of Figures

Figure 1.1 Sliding filament model of muscle movement.....	2
Figure 2.1 Schematic views of muscle fiber, myofibril and sarcomere at three different levels of magnification.....	6
Figure 2.2 Structure of myosin molecule.....	7
Figure 2.3 Structure of thin actin filament.....	8
Figure 2.4 The Lymn-Taylor cycle [18]. The myosin cross-bridge is bound to actin in the rigor, 45° “down” position (state 1). ATP binds, which leads to very fast dissociation from actin (state 2). The hydrolysis of ATP to ADP and P <sub>i</sub> leads to a return of the myosin cross-bridge to the 90° “up” position, whereupon it rebinds to actin (state 4). This leads to release of the products and a return to state 1. In the last transition, actin is “rowed” past myosin .....	9
Figure 2.5 the major change in the cross-bridge is confined to the distal part, which moves as a lever arm [23] .....	10
Figure 2.6 Schematic depiction of the Michael addition reaction [55].....	13
Figure 3.1 (a ) UV absorbance of bp on 4-np at different pH values and (b) Comparison of bp and pap on 4-np at pH 7 .....	21
Figure 3.2 bp kinetics and confirmation of substrate (dephosphorylated protein is casein kinase substrate).....	22
Figure 3.3 (a) Dry cross-linked sample as-molded; (b) hydrated gel at pH 7 .....	23
Figure 3.3 Hydrated gel at (c) pH 9; (d) pH 11 .....	24
Figure 3.3 Hydrated gel at (e) pH 13 and (f) pH 3 .....	25
Figure 3.4 (a) Contraction behavior of cross-linked casein gel via bp; (b) Dephosphorylation reaction and (c) Contraction cycle with constant pH adjustment to 9.....	28
Figure 3.5 Polymeric acid behavior: (a) dry protein; (b) hydrated protein at pH 7; (c) hydrated protein at pH 13; and (d) hydrated protein at pH 3 .....	30
Figure 3.6 Proposed model of dephosphorylation process with bp at neutral pH ..	31
Figure 4.1 Experimental protocol to demonstrate one cycle of the protein machine	36
Figure 4.2 Normalized UV-Visible absorbance of casein phosphorylation reaction. .....	37
Figure 4.3 Dephosphorylation and re-phosphorylation cycle of casein gel. Average volume change is blue line and average pH is red line.....	39
Figure 4.4 Casein gel volume change in water with the same pH adjustment as in Figure 3.4(d) .....	40
Figure 4.5 FT-IR spectra showed Amide I shift. Red: native casein cross-linked with DVS; blue: same sample dephosphorylated; green: same sample re- phosphorylated.....	41
Figure 4.6 FT-IR spectra demonstrated dephosphorylation and re-phosphorylation reactions .....	42
Figure 4.7 Schematic representation of casein micelle [19]. Polyelectrolyte "hairs" provide steric stabilization. The interaction between the hairs is modeled as a square-well adhesion of depth $\epsilon$ and width $\Delta$ .....	44
Figure 4.8 Illustration of protein machine expansion and contraction cycle.....	45

Figure 4.9 Estimation of elastic contribution to free energy .....	48
Figure 4.10 Estimation of elastic free energy efficiency.....	48

# CHAPTER 1

## **Introduction**

Our body never stops changing chemical energy to mechanical work at mild conditions of pH 7, 37°C, physiological ionic strength, and standard pressure. Due to adenosine triphosphate (ATP) hydrolysis, 30.5 kJ/mol [1] of energy is released and a fleet of biochemical reactions are triggered which drive the muscle to move.

Two fibrous proteins constitute the muscle sliding system. Actin and myosin lie parallel to each other and connect through a myosin head in the relaxed state. Stimulation of exocytosis leads to release of ATP which is stored within vesicles near the presynaptic membrane into the extracellular space [2]. Then the myosin head prefers to leave actin and react with ATP. Myosin and actin now slide over each other by a relative distance of  $\Delta x$  as shown in Figure 1. Once present extracellularly with a half-life measured in seconds, ATP is subject to a complex array of potent nucleotidases and other hydrolytic activities, which degrade ATP and generate ADP and phosphate ions,  $P_i$  [3]. After that, the ADP will leave the myosin head allowing the two proteins to return back to their original connected state. Although only 20% of the chemical energy in ATP is directly converted to muscle movement, this complex “sliding filament” mechanism is fairly efficient because the 80% lost chemical energy is used to maintain body temperature for basal metabolic processes [4].



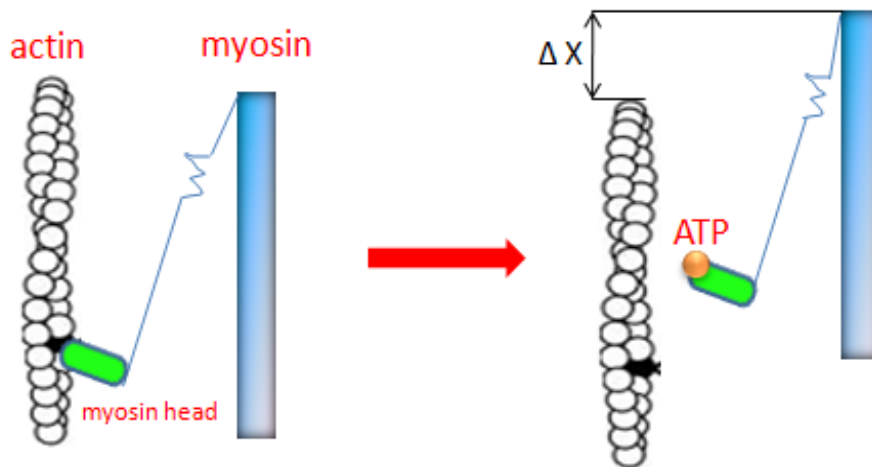


Figure 1.1 Sliding filament model of muscle movement

For engineering applications, directly mimicking muscle is not a good idea. Friction is the largest loss in the system followed by molecular conformational changes within the protein [4, 5, 6]. We therefore hypothesize that reducing the number of peptides to one and utilizing a protein able to recover its conformational losses (a “resilient” protein) will minimize losses in an engineered protein motor. Our initial vision is a protein system that undergoes a volume change at standard conditions to minimize energy inputs and can fully recover its volume through multiple cycles.

Therefore, the first goal is to synthesize a protein motor *in vitro*. Casein, a phosphoprotein, is reacted with divinyl sulfone (DVS) using a nucleophilic addition reaction known as the Michael addition which allows us to cross-link and modify the protein at standard conditions to greatly reduce the possibility of damaging the protein. The obtained cross-linked casein is stretched by negatively charged phosphate ions,  $P_i$ , covalently bound to the polymer backbone. So, when phosphorylated, the polymer behaves like a polymeric acid able to respond to pH or ionic strength change. A polymeric acid can change volume as the solution properties change, which is difficult to do in practice. The second goal is to demonstrate protein motor movement under more realistic biological conditions. To operate at standard conditions and to simulate a natural system where solution properties do not change, we propose a contraction by releasing  $P_i$  from the polymer using phosphatase enzyme, a reaction known as dephosphorylation.  $P_i$

ions are re-attached to the protein by a kinase enzyme when ATP is introduced, a reaction known as phosphorylation. This expands the protein motor back to its original state.

The resulting protein gel could be applied as a fundamental component in a variety of therapeutic applications, for example tissue engineering and pH controlled drug delivery. In tissue-engineering scaffolds, our protein gel is favorable because of its high water content, biocompatibility and biodegradability. Our protein hydrogel can readily serve to deliver signal to the cells, act as support structures for cell growth and function, and provide space filling [7]. Being a typical polymeric acid, our protein gel could be exploited as a drug delivery vehicle especially colon-specific delivery. The pH values in the gastrointestinal tract (GIT) vary in the stomach and small and large intestines. So during its passage through the upper GIT, the polymer is contracting in acidic media protecting the drug from rapid degradation and adsorption and swelling at higher pH releasing the drug to targeting sites in the lower GIT [8]. The unique feature of the protein machine is that it is not just a polymeric acid but able to respond to enzymes and convert chemical energy to mechanical work at neutral pH. Therefore, the protein machine can respond to phosphatases and kinases and may be a sensitive measure of their presence. The protein machine can respond to ATP. In its simplest incarnation, the protein machine could simply be used as a unique engine or transducer.

## 1.1 References:

1. Guynn, R. W., and R. L. Veech, The equilibrium constants of the adenosine triphosphate hydrolysis and the adenosine triphosphate-citrate lyase reactions. *J. Biol. Chem.*, 248:6966-6972, 1973
2. Burnstock G. Historical review: ATP as a neurotransmitter. *Trends Pharmacol Sci*, 27(3):166–17, 2006
3. Picher M, Burch LH, Boucher RC. Metabolism of P2 receptor agonists in human airways: implications for mucociliary clearance and cystic fibrosis. *J Biol Chem*, 279 (19), 20234–20241, 2004
4. Bormuth, V.; Varga, V.; Howard, J.; Schaffer, E., Protein friction limits diffusive and directed movements of kinesin motors on microtubules. *Science*, 325, 870-873, 2009
5. Laakso, J. M.; Lewis, J. H.; Shuman, H.; Ostap, E. M., Myosin I can act as a molecular force sensor. *Science*, 321, 133-136, 2008
6. Huxley, H. E., Neil B. Ingels, *The Molecular Basis of Force Development in Muscle*, J., Ed. Palo Alto Medical Research Foundation: Palo Alto, p 1-13, 1979
7. Peppas, N. A.; Hilt, J. Z.; Khademhosseini, A.; Langer, R. *Adv. Mater. Hydrogels in Biology and Medicine: From Molecular Principles to Bionanotechnology*. 18, 1345-1360, 2006
8. V.R. Sinha, R. Kumria, Polysaccharides in colon-specific drug delivery, *International Journal of Pharmaceutics*, 224, 19–38, 2001

## CHAPTER 2

### Literature review

#### 2.1 Muscle protein filament

##### 2.1.1 Structure of sarcomere

The sarcomere is the basic unit of muscle's cross-striated myofibril that causes a sliding motion [1]. The dark A band and light I band comprise each sarcomere unit and also make the interval banding appearance in the sarcomere. The A band has a lighter zone in the middle area called the H zone. There is a dark, thin Z line in the center of every I band as depicted in Figure 2.1 b. The unit between two Z lines is defined as one sarcomere unit, which is in the form of a cross-bridge constituted by the thin filament actin and the thick filament shown in Figure 2.1 c.

Although the fibrous thin actin and thick myosin are the main structural proteins in the system, actin and myosin alone cannot assume all of the responsibilities of muscle motion. Other proteins also play key roles in the sliding system. For example, in the thin filament, tropomyosin and troponin coupled with actin serve to regulate the interaction between actin and myosin. Tropomyosin and troponin lie along the entire length of the thin filaments. Similarly, in the thick filament, several proteins are associated with myosin like M-band protein [2, 3, 4], C-protein [5, 6, 7] and other less studied proteins, which are lying in specific regions rather than spread along the entire filament. The functions of these exact proteins are under study.

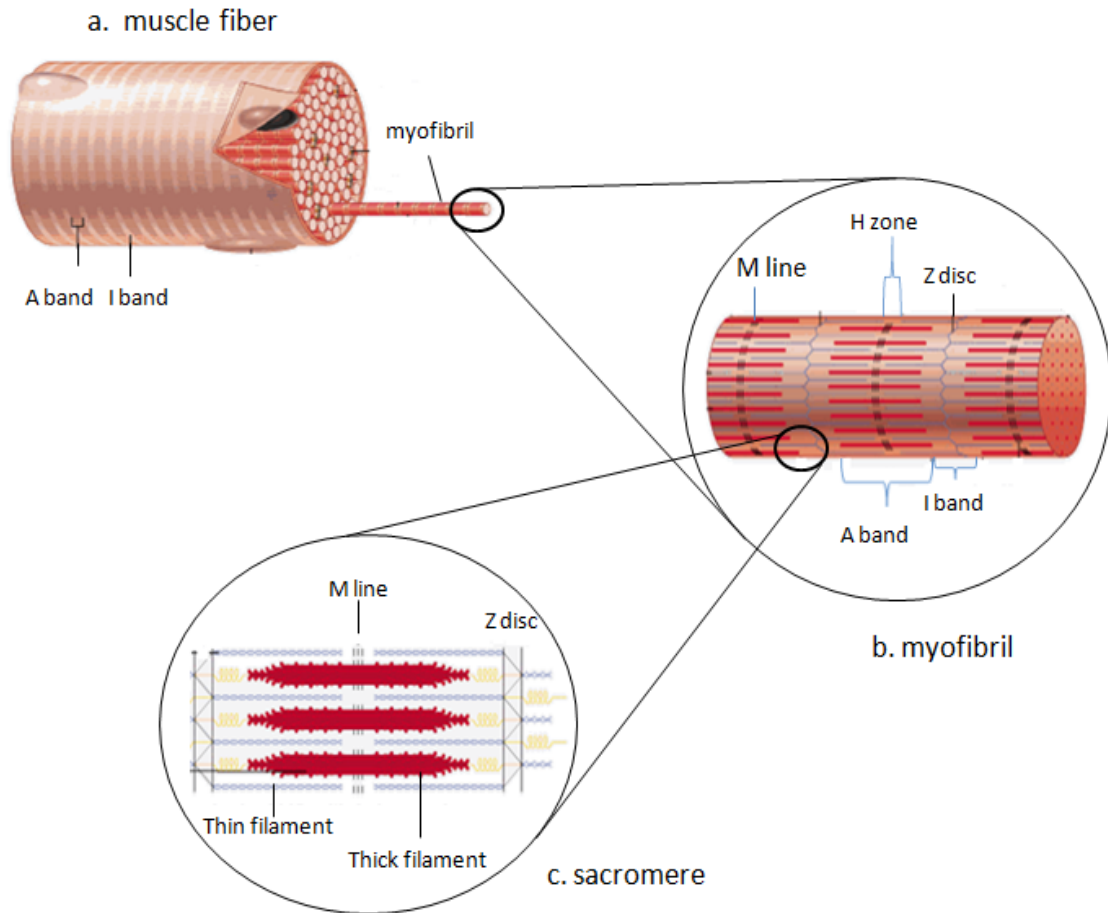


Figure 2.1 Schematic views of muscle fiber, myofibril and sarcomere at three different levels of magnification

### 2.1.2 Myosin filament

The length of the myosin filament among vertebrate striated muscles is 1.5  $\mu\text{m}$  [8, 9]. The middle portion of the thick filament is smooth but the surface is rough. The surface features of the two portions correspond to their functions. The rough surface facilitates the interaction of the myosin filament with the neighboring actin filaments [10].

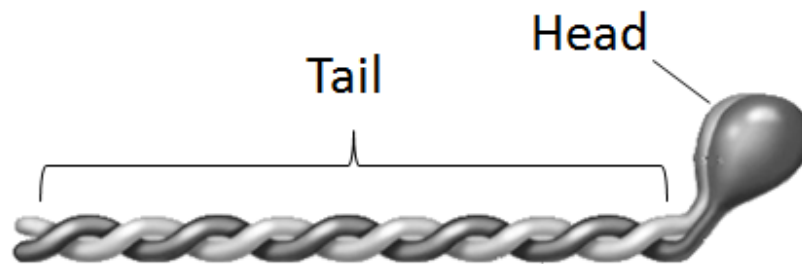


Figure 2.2 Structure of myosin molecule

The myosin molecule is divided into two essential parts, a long rod tail and a globular region at one end as shown in Figure 2.2. The rod portion is insoluble and the globular portion carries the adenosine triphosphatase (ATPase) and actin combining activity [11]. The insoluble rod portion allows myosin molecules to aggregate to form the shaft of the filament and the soluble globular portion works as an extended cross-bridge for interaction with neighboring actin filaments. Interaction of ATP with the globular portion of the myosi, results in sliding between the filaments and shortening of the muscle [12].

### 2.1.3 Actin filament

There is no big difference found in the structure of actin filaments of various cells so far. Typically, two helically wound strands which are around 360-370 nm in every cross-over repeat compose a thin actin filament backbone. The helically wound strands are made up of 13-14 spherical monomers in each cross-over unit [13]. Rod-shaped tropomyosin and globular troponin lying within the thin filament play important roles in the interaction of myosin and

actin. 400 nm long tropomyosin is located within the grooves between two actin strands and troponin is seated on tropomyosin with intervals of about 380 nm [14].

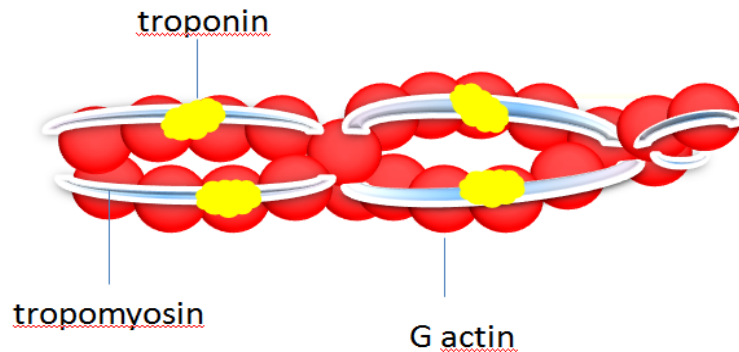


Figure 2.3 Structure of thin actin filament

#### 2.1.4 Molecular mechanism of muscle movement

The principal of the muscle sliding movement in contraction and expansion was discovered in the early 1950s. The molecular structure is based on thick filaments (composed mainly by myosin) and thin filaments (composed mainly by actin) [15].

The sliding filament model for muscle contraction envisions two steps: first, the myosin binds to the actin filament at the cross-bridge head; second, the myosin filament experiences a swinging motion that “rows” along the actin filament [16]. ATPase in the myosin head is product-inhibited with an active site and mechanism similar to that of the G-proteins [17]. When the myosin head binds to actin, the ATPase is strongly stimulated which is a nucleotide actor for myosin. If the nucleotide actor is not activated, the actin filament binds the myosin cross-bridge to form the “strong” or “rigor” complex as depicted in Fig 2.4.1. The actomyosin complex will disassemble immediately when ATP binds to the myosin cross-bridge on the ATPase site where the ATP is hydrolyzed to induce a stable myosin-products complex (ADP and  $P_i$ ). After that, actin recombines with the myosin-products complex and releases the products. So the binding conformation of the actomyosin complex returns back to its original state [18]. When it recombines with actin, the cross-bridge head experiences another conformational change allowing ADP and  $P_i$  to be released, which also brings about the rowing-like stroke (this elemental event is referred to as the “power stroke”).

Though most textbooks have accepted the swinging-cross-bridge hypothesis of muscle contraction theory, it is difficult to visualize a bridge during the swing. More recently, with the development of new X-ray techniques [19], scientists performed low-angle time-resolved low angle X-ray diffraction on contracting frog muscle that provided evidence of cross-bridge movement [20, 21]. However, it failed to envision cross-bridge movement in large detail due to insufficient resolution. With the advent of spectroscopic and structural observations [22], the swinging cross-bridge model underwent an evolution and developed into a swinging-lever arm hypothesis. It supports the bulk of the cross-bridge model but without sliding on the surface during the power stroke. The distal (C-terminal) part of the myosin cross-bridge moves like a lever arm bringing large movements as shown in Figure 2.5.

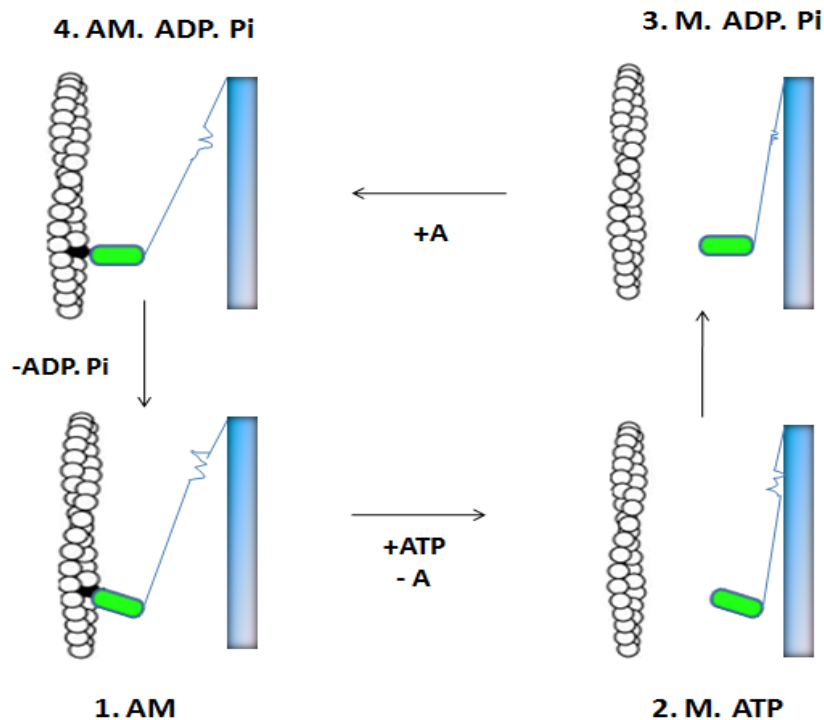


Figure 2.4 The Lymn-Taylor cycle [18]. The myosin cross-bridge is bound to actin in the rigor, 45° "down" position (state 1). ATP binds, which leads to very fast dissociation from actin (state 2). The hydrolysis of ATP to ADP and P<sub>i</sub> leads to a return of the myosin cross-bridge to the 90° "up" position, whereupon it rebinds to actin (state 4). This leads to release of the products and a return to state 1. In the last transition, actin is "rowed" past myosin

Furthermore, it gradually became clear that the proportion of cross-bridges taking part in a contraction at any one time was only a small fraction of the total [23], which makes the registration of active cross-bridge movement doubly difficult.



The swinging lever arm can explain why few changes are observed in the cross-bridge orientation: only a small fraction of the cross-bridge mass moves during the power stroke. Gradually, it was further confirmed that at any one time there is always a small fraction of the total cross-bridges joined in a contraction [23]. This makes the active cross-bridge movement model not comprehensive.

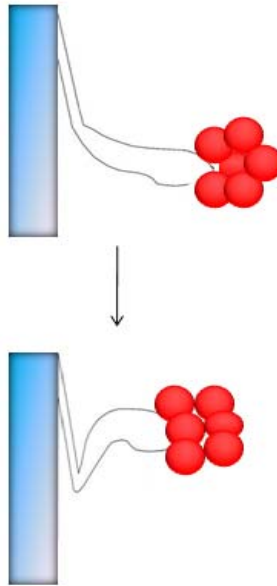


Figure 2.5 The major change in the cross-bridge is confined to the distal part, which moves as a lever arm [23]

## 2.2 Ionic polymer gel

In recent years, much attention has been directed to ionic polymer gels as “synthetic muscle”. Ionic polymer gels respond to small changes in solution ionic strength by swelling to different degrees [24]. “Ionic hydrogel” refers to a wide range of anionic, cationic, amphoteric [25], and zwitterionic [26] materials.

Polymeric networks containing ionic and/or hydrophobic moieties are responsive to environmental conditions. These environmental conditions include pH [27], pressure [28], ionic strength [29], temperature [30], magnetic fields [31], and many other external variables.

The pH-responsive gels, a subgroup of ionic polymer gels, have drawn interest for the potential for various novel applications, including drug delivery [32], immobilized enzyme systems, [33] and separation processes [34]. For example, Guderman and Peppas have

synthesized a pH sensitive interpenetrating network of poly(vinyl alcohol) and monoprotic acrylic acid [35]. This type of ionic gel can be ionized at the proper pH and undergoes a large volume change in response to variations in the pH of the swelling solution [36].

## 2.3 Synthesis of protein machine

### 2.3.1 Design principle of protein machine

As in other emerging fields, there is not a clear consensus as to what is necessary for a molecular machine and what differentiates them from other molecular devices. Many of the chemical systems first likened to motors and other machines were simply host–guest complexes in which the binding could be switched “on” or “off” by external stimuli such as light, temperature, ionic strength, or electrical charge [37-40]. Most were polymer gels due to their reversible size and shape change, thereby realizing macroscopic motion by integrating the deformation on a molecular level [41]. One of the earliest *in vitro* studies of motor protein mechanochemistry was the utilization of myosin molecules immobilized on a solid substrate to transport actin strands across the surface [42]. The potential application of these protein motors is the transport of nanoscale cargoes and consequently the challenges of controlling and directing the motion, as well as capturing and releasing molecular materials, are actively being pursued. Similar systems have been developed on the muscle sliding filaments system. In the presence of ATP, a chemically cross-linked actin gel could move over a cross-linked myosin gel.

Here we choose to make a molecular machine that does not work from an electrical, heat, pH, or ionic strength input but from an ATP input only, more similar to real muscle [43]. The material is macroscopically a protein polymer gel. Motion is realized by overall chain deformation caused by phosphorylating and dephosphorylating the protein. When phosphorylated, the negative charges on the phosphate ions repel each other and swell the gel. Once dephosphorylated, the gel would lose negative charges and contract. Therefore, the things required to build the proposed protein machine are a protein capable of being phosphorylated, a method to prepare a gel of the protein without significantly changing or damaging it, and readily available enzymes to phosphorylate and dephosphorylate the protein.

### 2.3.2 Casein

Caseins, the major milk proteins in ruminants, are a family of four acidic phosphoproteins ( $\alpha_{s1}$ -,  $\alpha_{s2}$ -,  $\beta$ -, and  $\kappa$ -caseins) that are synthesized in the mammary gland in response to lactogenic hormones and other stimuli and form colloidal micelles in milk (for review, see [44]). Casein is easily obtainable and there is a large body of literature on mechanisms to phosphorylate and dephosphorylate it.

Casein has many desirable functional properties and is used extensively in the food industry. For example, because of their amphiphilic nature and flexible structure, caseins have excellent solubility and capacity to form films. The protein interacts with other components in the solution either to remain soluble or to form protein films at phase interfaces to create an emulsion or foam.

Bovine whole casein is a mixture of four phosphoproteins,  $\alpha_{s1}$ -,  $\alpha_{s2}$ -,  $\beta$ -, and  $\kappa$ -caseins, which are present in a ratio of 3:1:3:1 and have 8 to 9, 10 to 14, 5, and 1 phosphate group per molecule, respectively [45]. The negatively charged phosphate groups bound to the caseins can be removed enzymatically with acid phosphatase [46, 47, 48], alkaline phosphatase [49], and phosphoprotein phosphatase [50, 51, 52].

The removal of the phosphate groups from casein alters some of the physical and functional properties of the protein, thereby changing the way in which the caseins associate and form micelles [53]. Calcium-binding capacities of dephosphorylated (DP) whole  $\alpha_s$ -caseins are significantly lower than those of the native caseins [54]. The DP whole casein is more readily hydrolyzed by pepsin than native casein.

### 2.3.3 Michael addition

The Michael addition reaction, which is also commonly termed conjugate addition, has several advantages, like high functional group tolerance, a large host of polymerizable monomers and functional precursors as well as high conversions and favorable reaction rates. Therefore, as a polymer synthesis approach, it has gained increased attention [55, 56].

These unique features facilitate Michael addition reaction to find applications in a number of emerging technologies including biomedical applications such as gene transfection [57], cell

scaffolds [58] and tissue replacements [59]. Here, the Michael addition can be employed to cross-link casein to form a protein gel without damaging the protein structure.

The Michael addition reaction is simply the base-catalyzed addition of a nucleophile (Michael donor) to an activated  $\alpha, \beta$ -unsaturated carbonyl-containing compound (Michael acceptor) as shown in Figure 2.6. However, over the years, the scope of this reaction has evolved greatly to include a broad range of acceptors and the Michael-type additions of non-carbon donors.

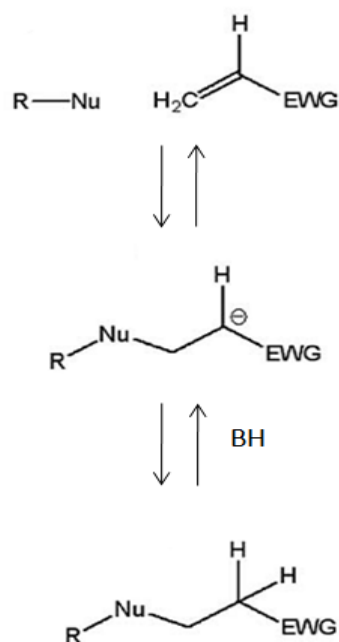


Figure 2.6 Schematic depiction of the Michael addition reaction [55]

The mild Michael addition reaction conditions are well-suited to biological applications such as protein derivitization because high temperatures, oxidizing radicals, and organic solvents are not feasible [59].

#### 2.3.4 Synthesis of protein machine

Native, phosphorylated casein is first cross-linked with divinyl sulfone (DVS) using the Michael addition. The reaction occurs at pH 10 and room temperature in water. The reaction is



where P is protein. This forms a protein gel capable of being highly swollen with water creating the environment necessary to dephosphorylate and re-phosphorylate the gel. The ability of DVS to cross-link polypeptide chains has been used previously to prepare dimers of bovine [60] and human [61] liver ribonuclease.

## 2.4 References:

1. Huxley, H. E., Structure. In *The Molecular Basis of Force Development in Muscle*, Neil B. Ingels, J., Ed. Palo Alto Medical Research Foundation: Palo Alto; pp 1-13, 1979
2. Weber A, Murray JM: Molecular control mechanisms in muscle contraction. *Physiol Rev* 53:612, 1973
3. Eaton B, Pepe FA: M band protein: two components isolated from chicken breast muscle. *J Cell Biol* 55:681, 1972
4. Masaki T, Takaiti : M-protein. *J Biochem* 75:367, 1974
5. Offer G: C-protein and the periodicity in the thick filaments of vertebrate skeletal muscle. *Cold Spring Harbor Symp Quant Biol* 37:87, 1972.
6. Pepe FA: The myosin filament: immunochemical and ultrastructural approaches to molecular organization. *Cold Spring Harbor Symp Quant Biol* 37:97, 1972
7. Pepe FA, Craig B. Offer G, Drucker B: Fluorescence and electron microscopy of myofibrils labeled with antibodies to myosin and C-protein. In preparation
8. Page S, Huxley HE: Filament lengths in striated muscle. *J Cell Biol* 19:369, 1963
9. Pepe FA: The structural components of the striated muscle fibril, *Biological Macromolecules Series: Subunits in Biological Systems*. Marcel Dekker, mc, New York, p 323-353, 1971
10. Huxley HE: Electron microscope studies on the structure of natural and synthetic protein filaments from striated muscle. *J Mol Biol* 7:281, 1963
11. Huxley, H. E. The double array of filaments in cross-striated muscle, *J. Cell, Biol.* 3(5): 631-648, 1957
12. Huxley H.E, Hanson J: Changes in the cross striations of muscle during contraction and stretch and their structural interpretation. *Nature* 173:973, 1954
13. Hanson J: Recent x-ray diffraction studies of muscle. *Q Rev Biophys* 1:177, 1968
14. Ebashi S: Calcium ions and muscle contraction. *Nature* 240:217, 1972
15. Hanson J, Huxley HE. The structural basis of contraction in striated muscle. *Symp Soc Exp Biol*, 9:228–264, 1995
16. Rezanowich, A., Yean, W.Q., Goring, D.A.I., High resolution electron microscopy of sodium lignin sulfonate. *J Apply Polymer Sci*, 8: p. 1801-1812, 1964
17. Kosikova, B., Zakutna, L., Joniak, D., Investigation of the lignin-sacharidic complex by electron microscopy. *Holzforschung*, vol 32: p. 15-18, 1978
18. Gilardi, G. and A.E.G. Cass, Associative and Colloidal Behavior of Lignin and Implications for Its Biodegradation in-Vitro. *Langmuir*, 9 (7): p. 1721-1726, 1993
19. Atalla, R.H. and U.P. Agarwal, Raman Microprobe Evidence for Lignin Orientation in the Cell-Walls of Native Woody Tissue. *Science*, 227(4687): p. 636-638, 1985
20. Sarkanen, S., et al., Associative Interactions between Kraft Lignin Components. *Abstracts of Papers of the American Chemical Society*, 187(Apr): p. 24-Cell, 1984
21. Sarkanen, S., et al., Lignin .19. Kraft Lignin Component Conformation and Associated Complex Configuration in Aqueous Alkaline-Solution. *Macromolecules*, 15(4): p. 1098-1104, 1982
22. Cathala, B., et al., Evaluation of the reproducibility of the synthesis of dehydrogenation polymer models of lignin. *Polymer Degradation and Stability*, 59(1-3): p. 65-69, 1998
23. Tanahashi, M., T. Aoki, and T. Higuchi, Dehydrogenative Polymerization of Monolignols

- by Peroxidase and H<sub>2</sub>O<sub>2</sub> in a Dialysis Tube .2. Estimation of Molecular-Weights by Thermal Softening Method. *Holzforschung*, 36(3): p. 117-122, 1982
24. S.Hirotsu, Y. Hirokawa, T. Tanaka, Volume-phase transitions of ionized N-isopropylacrylamind gels, *J. Chem. Phys*, 87,1392, 1987
  25. A. E. English, S. Mafe, J. A. Manzanares, X. Yu, A. Y. Grosberg, T. Tanaka, Equilibrium swelling properties of polyampholytic hydrogels , *J. Chem. Phys*, 104, 8713, 1996
  26. W. Xue, M. B. Huglin, A. T. Russell, Unusual behaviour of crosslinked and linear forms of a zwitterionic polymer in aqueous alkali , *Macromol. Rapid Commun*, 20, 239, 1999
  27. Kuo JH, Amidon GL, Lee PI. pH-Dependent swelling and solute diffusion characteristics of poly(hydroxyethyl methacrylate-co-methacrylic acid) hydrogels. *Pharm Res*, 5: 592-597, 1988
  28. Lee KK, Cussler EL, Marchetti M, McHugh MA. Pressure dependent phase transitions of hydrogels. *Chem Eng Sci*, 45: 766-767, 1990
  29. I. Ohmine, T. Tanaka, Salt effects on the phase transition of ionic gels, *J. Chem. Phys*, 77, 5725, 1982
  30. T. Tanaka, Collapse of gels and the critical endpoint, *Phys. Rev. Lett.* 1978, 40, 820.
  31. M. Zrinyi, Intelligent polymer gels controlled by magnetic fields, *Colloid Polym. Sci*, 278, 98, 2000
  32. Scranton, A. B.; Rangarayan, B.; Klier, Biomedical applications of polyelectrolytes, *J. Adv Polym Sci*, 122, 3, 1995
  33. Putman, P.; Kopecek, Polymer conjugates with anticancer activity, *J. Adv Polym Sci*, 122, 55, 1995
  34. Karadag , E.; Saraydin, D.; Guven, O, Effect of pH, Ionic Strength, and Temperature on Uranyl Ion Adsorption by Poly(N-vinyl 2-pyrrolidone-g-tartaric Acid) Hydrogels, *Sep Sci Technol*, 30, 3747, 1995
  35. Gudeman, L. F.; Peppas, N. A., Preparation and characterization of pH-sensitive, interpenetrating networks of poly(vinyl alcohol) and poly(acrylic acid)*J Appl Polym Sci*, 55, 919, 1995
  36. M. J. Molina, M. R. Go ´mez-Anto ´n, I. F. Pie ´rola, pH-Dependence of the Swelling Capacity of Poly(N-vinylimidazole) Hydrogels, *Macromol. Chem. Phys*, 203, No. 14, 2002
  37. Takahashi, N. and T. Koshijima, Molecular-Properties of Lignin-Carbohydrate Complexes from Beech (*Fagus-Crenata*) and Pine (*Pinus-Densiflora*) Woods. *Wood Science & Technology*, 22(2): p. 177-189, 1988
  38. Kuhn, W.; Hargitay, B.; Katchalsky, A.; Eisenberg, H., Reversible dilation and contraction by changing the state of ionization of high-polymer acid networks. *Nature*, 165, 514-516, 1950
  39. Hamlen, R. P.; Kent, C. E.; Shafer, S. N., Electrolytically activated contractile polymer. *Nature*, 206, 1149-1150, 1965
  40. Calvert, P., Hydrogels for soft machines. *Advanced Materials*, 21, 743-756, 2009
  41. Kakugo, A.; Shikinaka, K.; Ping Gong, J.; Osada, Y., Gel machines constructed from chemically cross-linked actins and myosins. *Polymer*, 46, 7759-7770, 2005
  42. Ferruti P, Bianchi S, Ranucci E, Chiellini F, Caruso V. Novel poly(amido-amine)-based hydrogels as scaffolds for tissue engineering. *Macromol Biosci*, 5:613–22, 2005
  43. Paxton, W. F.; Sundararajan, S.; Mallouk, T. E.; Sen, A., Chemical locomotion. *Angewandte Chemie International Edition*, 45, 5420-5429, 2006

44. Barakat, A., et al., Studies of xylan interactions and cross-linking to synthetic lignins formed by bulk and end-wise polymerization: a model study of lignin carbohydrate complex formation. *Plant*, 226(1): p. 267-281, 2006
45. Eigel, W. N., J. E. Butler, C. A. Emstrom, H. M. FmU, Jr., V. R. Harwalkar, R. Jenness, and R. M. Whitmy. Nomenclature of proteins of cow's milk: tifth nvision. *J. Dairy Sci.* 67:1599, 1984
46. Bingham, E. W. H. M. Fanell, Jr., and K. J. Dahl. Removal of phosphate groups from casein with potato acid phosphatase. *Biochim. Biophys. Acta* 429: 448, 1976
47. LiChan. E., and S. Nakai. Enzymic dephosphorylation of bovine casein to improve acid clotting properties and digestibility for infant formula. *J. Dairy Res.* 56:381, 1989.
48. Schmidt, D. G., and J. K. Poll. Properties of artificial casein micelles. 4. Influence of dephosphorylation and phosphorylation of the casein. *J Milk Dairy.* 43:53, 1989
49. Pearse, M. J.. P. M. Linklater, R. J. Hall, and A. G. Mackinlay. Effect of casein micelle composition and casein dephosphorylation on coagulation and syneremis. *J. Dairy Res.* 53:381, 1986
50. Aoki, T., N. Yamada, I. Tomita, Y. Kako. and T. ester phosphate groups by colloidal calcium phosphate. *Biochim. Biophys. Acta* 911:238
51. U Yoshikawa, M.. E. Sugimoto, and H. Chiba. Studies on the interaction between  $\alpha$  and  $\beta$ -caseins. *Agric. Biol. Chem.* 39:1843. 1975
52. Yun. S.. K. Ohmiya, S. Shimizu. Role of the phosphoryl group of B-casein in milk curdling. *Agric. Biol. Chem.* 46:1505. 1982
53. Bingham, E. W., H. M. Famll. Jr., and R. J. Carroll. Propertie of dephosphorylated a,l-casein. Precipitation by calcium ions and micelle formation. *Biochemistry* 11:2450, 1972
54. Yamauchi. K., S. Takemoto, T. Tsugo. Calcium-binding property of dephosphorylated caseins. *Agric. Biol. Chern.* 3154, 1967
55. Mather, B. D.; Viswanathan, K.; Miller, K. M.; Long, T. E., Michael addition reactions in macromolecular design for emerging technologies. *Progress in Polymer Science*, 31, 487-531, 2006
56. Vernon B, Tirelli N, Bachi T, Haldimann D, Hubbell J. Waterborne, in situ crosslinked biomaterials from phase-segregated precursors. *J Biomed Mater Res* 2003, 64A:447–56.
57. Richardson SCW, Patrick NG, Stella Man YK, Ferruti P, Duncan R. Poly(amidoamine)s as potential nonviral vectors: ability to form interpolyelectrolyte complexes and to mediate transfection in vitro. *Biomacromolecules*, 2:1023–8, 2006
58. Ferruti P, Bianchi S, Ranucci E, Chiellini F, Caruso V. Novel poly(amido-amine)-based hydrogels as scaffolds for tissue engineering. *Macromol Biosci*, 5:613–22, 2006
59. Elbert DL, Pratt AB, Lutolf MP, Halstenberg S, Hubbell JA. Protein delivery from materials formed by self-selective conjugate addition reactions. *J Control Release*, 76: 11–25, 2001
60. Kakugo, A.; Shikinaka, K.; Ping Gong, J.; Osada, Y., Gel machines constructed from chemically cross-linked actins and myosins. *Polymer*, 46, 7759-7770, 2005
61. Kakugo, A.; Shikinaka, K.; Ping Gong, J.; Osada, Y., Gel machines constructed from chemically cross-linked actins and myosins. *Polymer*, 46, 7759-7770, 2005



## CHAPTER 3

# Casein-based protein machine and demonstration of contraction cycle

### 3.1 Introduction

We have developed a protein machine using a cross-linked casein gel. The protein was cross-linked by reacting electrophilic vinyl groups on divinyl sulfone (DVS) with nucleophilic amines on casein. The reaction was performed at pH=10, 298 K, and 101 kPa which eliminated the risk of damaging the protein. After reaction, the solution was poured into molds 1 cm × 0.5 cm × 0.5 cm and dried. The obtained gel behaved like a polymeric acid, expanding at high pH and contracting at low pH.

To operate at standard conditions, appropriate enzymes need to be identified to perform the phosphorylation and dephosphorylation reactions. In this chapter the dephosphorylation reaction and concurrent contraction of the protein machine will be explored. First, the dephosphorylation ability of bovine phosphatase (bp) and potato acid phosphatase (pap) at pH 7 were compared via UV-Visible spectroscopy at 410 nm. The results showed that bp was more effective than pap at physiological pH. Using bp, the cross-linked casein gel was dephosphorylated. An immediate pH drop and a gel contraction as much as 90% were observed. In order to eliminate the contribution of pH to the contraction, we constantly adjusted the pH back to 9 where  $\text{pH} > \text{pK}_a^{2-}$  until the volume stopped changing. The pH contribution resulted from the fact that the protein was negatively charged and therefore lost charge with decreasing pH. The contraction as a result of enzyme-driven dephosphorylation was only 70%. Therefore, the majority of contraction came from dephosphorylation with a smaller contribution from screening of negative charge on the rest of the protein

## 3.2 Materials and methods

### 3.2.1 Materials

4-nitrophenyl phosphate (4-np, tablet), bovine phosphatase (bp, 20 mg protein/ml, 6202 units/mg protein), potato acid phosphatase (pap, lyophilized powder, 3.0-10.0 units/mg solid), casein, casein kinase substrate, and divinyl sulfone (DVS, 97% with 0.05% hydroquinone) were obtained from Sigma-Aldrich and used without further modification.

### 3.2.2 Dephosphorylation activity of bovine phosphatase and potato acid phosphatase on 4-np

0.4326 g 4-np was dissolved into 333.3 ml de-ionized (DI) water. 0.0001 g pap or 5  $\mu$ l bp was then added. The reaction was run at 38°C for 0, 1, 3, 5, 10, 30, 50, and 100 minutes. The reaction was terminated by adding 0.25 M NaOH to 1 ml samples collected in cuvettes for UV-Visible spectroscopy. The UV-Visible absorbance at 410 nm was measured to assess phosphatase kinetics according to Deal et al [1]. Controls samples were solutions with enzyme and 4-np only and showed no absorbance.

### 3.2.3 Dephosphorylation of uncross-linked casein and casein kinase substrate with bovine phosphatase (bp)

As will be shown in the results, bovine phosphatase provided the best dephosphorylation at pH 7-9. Dephosphorylation with bovine phosphatase was carried out on native, uncross-linked, phosphorylated casein or casein kinase substrate using the method of Bingham et al [2] with modification (pH 7, 38°C). Casein kinase substrate is commercially available dephosphorylated casein. 0.125 g casein or casein kinase substrate was added into 50 ml DI water with 0.0001 g bp. The reaction was performed for 0, 30, 60, 90, and 120 minutes and terminated by adding 3 ml of 0.25 M NaOH for every 1 ml solution sampled.

### 3.2.4 Cross-linking casein with DVS

0.25 g whole casein was dissolved in 50 ml DI water. The solubility of casein was poor so pH was adjusted to and maintained at  $10 \pm 0.5$  by continuous addition of 0.1M NaOH [3]. The solution was allowed to mix for 24 hours so that all of the casein was completely dissolved and pH was stable. 10% w/w DVS (21.2  $\mu$ l) was added and stirred for 24 h at ambient conditions and pH 10 [4]. The solution was then dialyzed against pure water for 24 hours changing the water every 12 hours. The dialyzed liquid was poured into 1 cm  $\times$  0.5 cm  $\times$  0.5 cm molds and dried under a fume hood for 48 hours so that drying was not very rapid so as to potentially induce protein aggregation. Samples were stored under vacuum until tested.

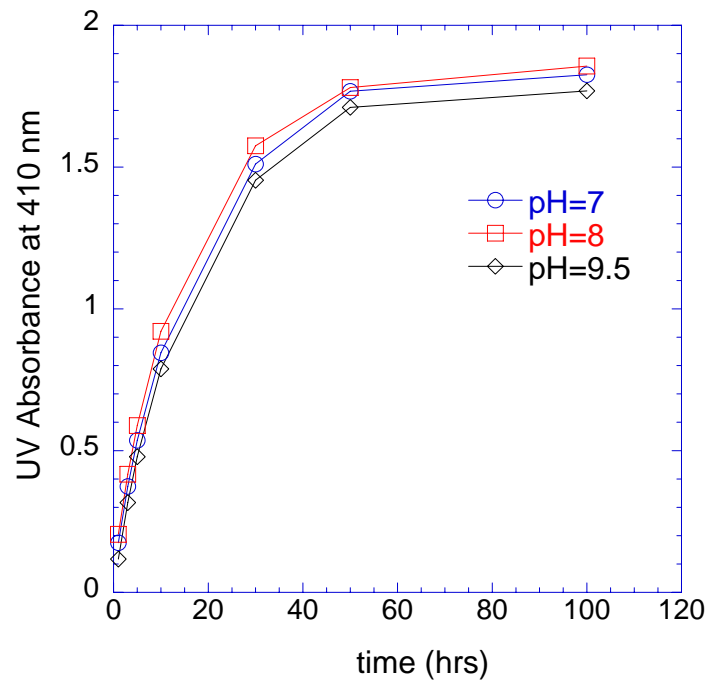
### 3.2.5 Measurement of contraction cycle

Dry, as-molded cross-linked casein samples were placed into 300 ml DI water and hydrated for two hours at pH 9 to produce the hydrated gel. This time was found to be sufficient to reach maximum expansion. 5  $\mu$ l bp was now added and the volume change monitored as a function of time. Concurrently, the same experiment was performed but pH was continually adjusted to 9.

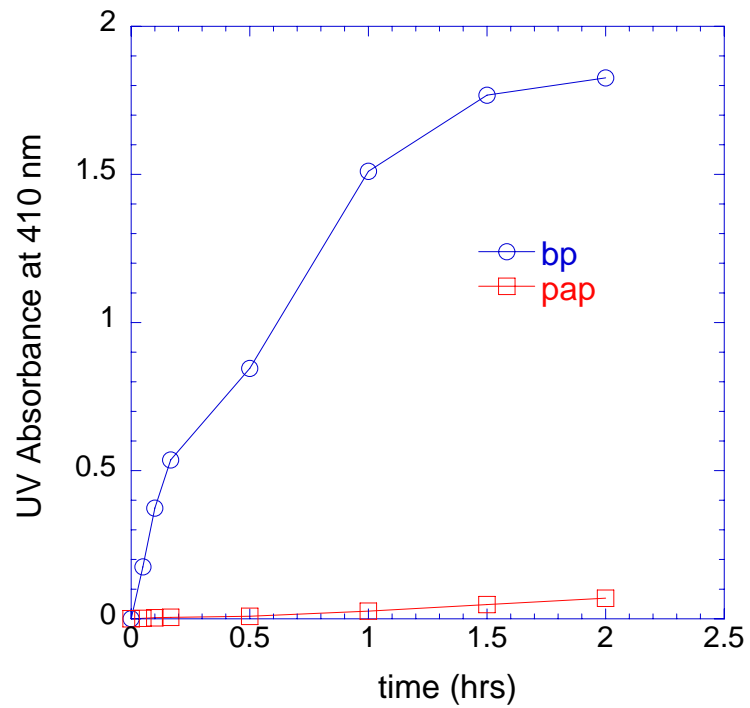
## 3.3 Results

### 3.3.1 UV-Visible results of dephosphorylation activity of bovine phosphatase and potato acid phosphatase

Figure 3.1 shows the results for dephosphorylation of casein and casein kinase substrate using bp and pap. Bovine phosphatase was very efficient at pH 7-9 displaying Michaelis-Menten type behavior.



(a)



(b)

Figure 3.1 (a) UV absorbance of bp on 4-np at different pH values and (b) Comparison of bp and pap on 4-np at pH 7

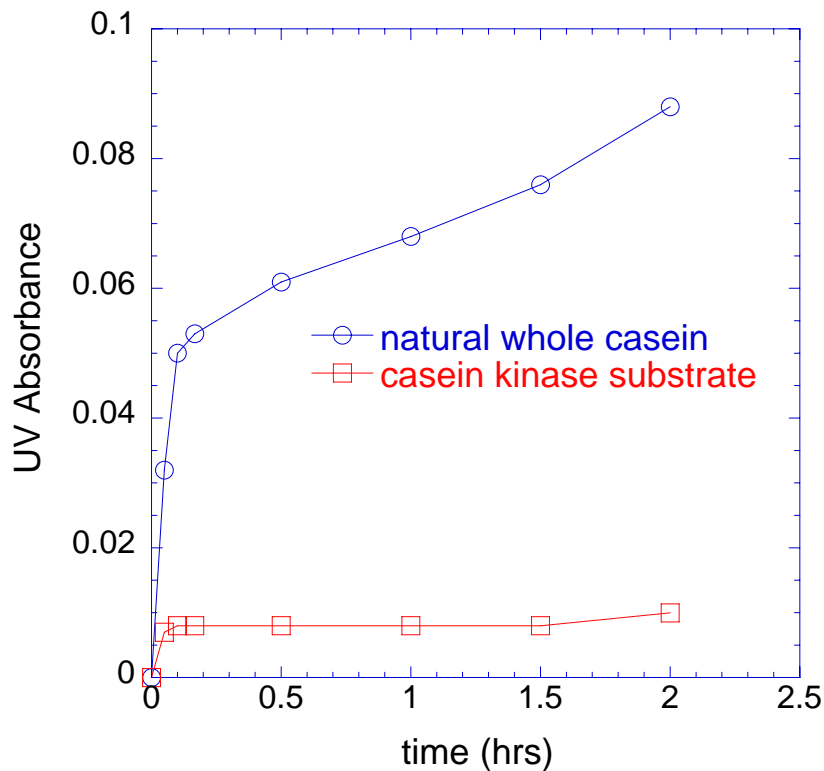


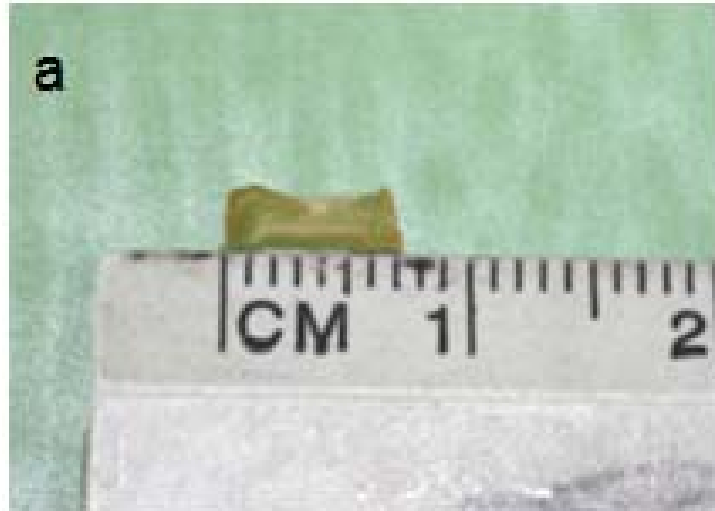
Figure 3.2 bp kinetics and confirmation of substrate (dephosphorylated protein is casein kinase substrate)

Fig 3.2 indicated that bp was able to work effectively on native, phosphorylated casein with Michaelis-Menten kinetics. Dephosphorylation was fast in the first 5 minutes and then slowed down in the following 120 minutes. No change was observed with dephosphorylated casein (casein kinase substrate) confirming it was sufficiently dephosphorylated as-received.

### 3.3.2 Protein machine and its characterization

The UV-Visible results revealed that bp was the most efficient enzyme for dephosphorylation at physiological and near physiological conditions. An example of a dry, cross-linked native casein sample is shown in Figure 3.3 (a). After 2 hours of hydration, the material appeared as shown in Figure 3.3 (b). Figures 3.3 (c)-(f) show that

the gel behaved as a typical polymeric acid, expanding at high pH and contracting at low pH.



(a)



(b)

Figure 3.3 (a) Dry cross-linked sample as-molded; (b) hydrated gel at pH 7



(c)



(d)

Figure 3.3 Hydrated gel at (c) pH 9; (d) pH 11



(e)



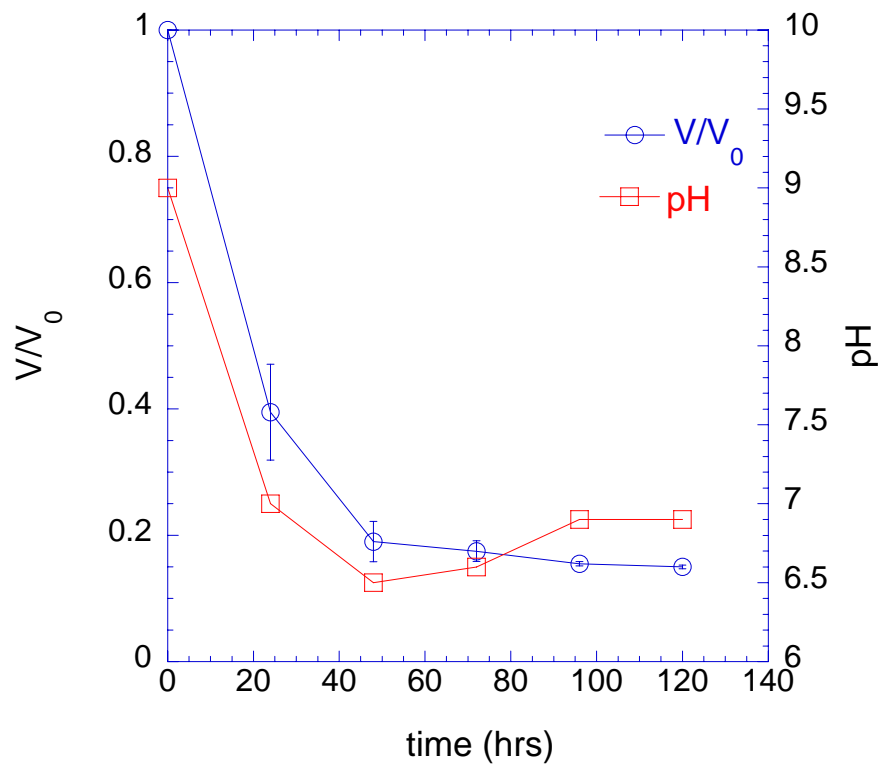
(f)

Figure 3.3 Hydrated gel at (e) pH 13 and (f) pH 3

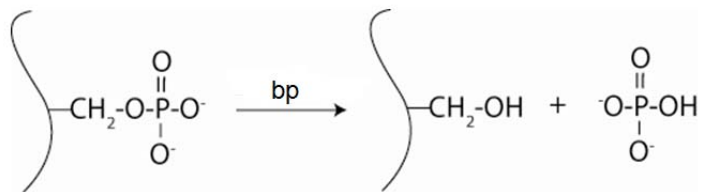


When phosphorylated, the gel acted just like a polymeric acid able to respond to pH or ionic strength change. Phosphate ions by themselves,  $P_i$ , had 3  $pK_a$ 's (2.1, 7.2, and 12.7) because of the  $3^-$  valency and the protein had  $pI \sim 4.6$  [3]. When phosphate groups were attached to the protein backbone via hydroxyl groups on Ser/Thr, there were 2  $pK_a$ 's (2.1, 7.2). The swelling results correlated well with the 2  $pK_a$ 's of  $P_i$ . At low pH near  $pK_a^-$  there was very little negative charge on phosphate ions and the gel was in its most contracted state. At neutral pH close to  $pK_a^{2-}$ , the highly negatively charged phosphate groups on casein repelled each other and expanded the gel. Very little change in volume was observed between pH 7 and 11 but further expansion was observed at pH 13. The increased expansion at highly basic solution was caused by the deprotonation of amine groups on amino acid side chains. The gels were stable in aqueous solution and did not exhibit hydrolytic degradation over the course of these experiments.

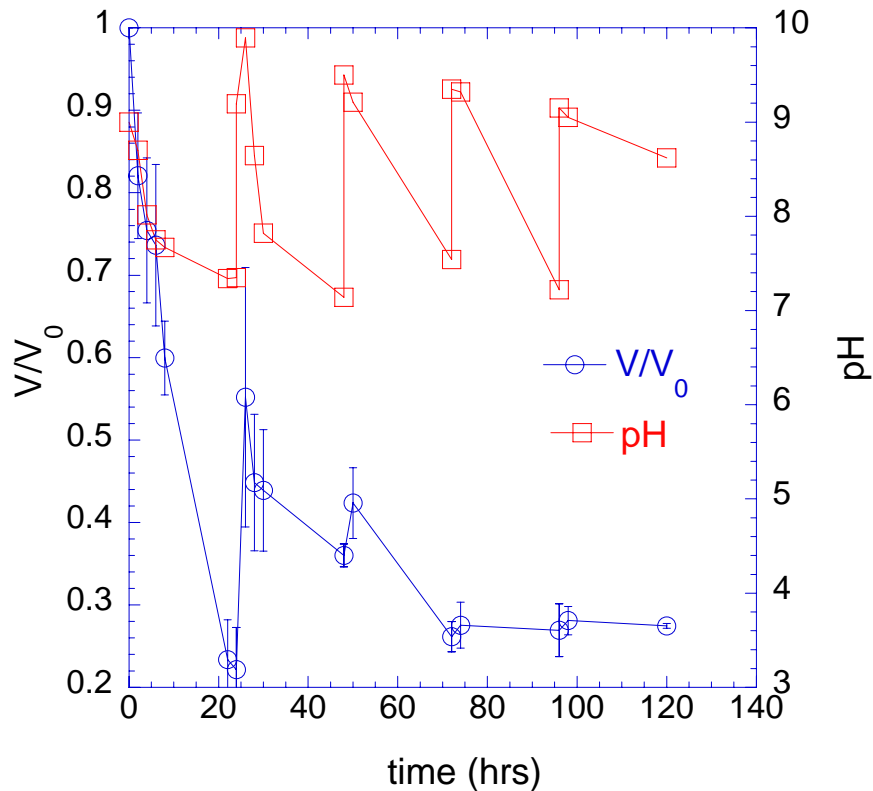
Bovine phosphatase (bp) was added to the hydrated cross-linked protein in solution. Very quickly, the pH of the solution dropped with a concurrent  $\sim 90\%$  contraction of the protein as shown in Figure 3.4 (a). The released  $P_i$  detached from the protein backbone and lowered the pH as shown in Figure 3.4 (b). Clearly there was proton release resulting in pH decrease. In this experiment, overall volume change originated from loss of negative charge and pH decrease. A concurrent experiment was performed with constant pH adjustment back to 9 and the results are shown in Figure 3.4 (c). At constant pH  $> pK_a^{2-}$ , the total contraction was  $\sim 70\%$  indicating that most but not all of the contribution to volume change was from loss of phosphate groups. The adjustment of pH back to 9 not only allowed for the assessment of the contributions from phosphate ions and other negative charge on the protein, but allowed the bp dephosphorylation reaction to continue to run to completion as evidenced by the change in volume until long time was reached.



(a)



(b)



(c)

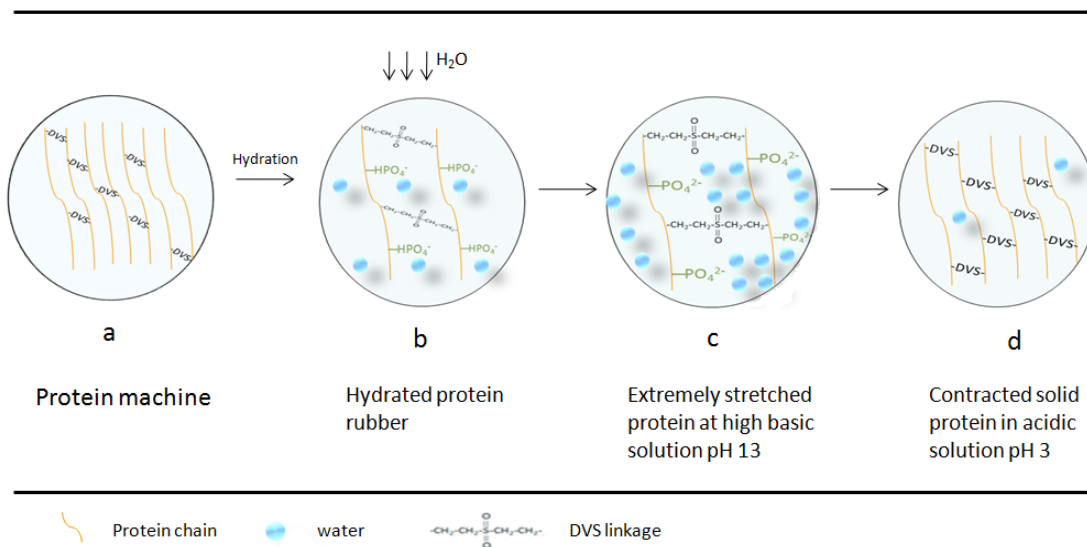
Figure 3.4 (a) Contraction behavior of cross-linked casein gel via bp; (b) Dephosphorylation reaction and (c) Contraction cycle with constant pH adjustment to 9

### 3.4 Discussion

It has been reported that although acid and alkaline phosphatases are distinct enzymes [6], they usually occur together and have somewhat similar properties except for pH effects. In our test, bovine phosphatase, rather than potato acid phosphatase, was the predominant protein phosphatase under physiologically relevant conditions. However, the observed change in pH with dephosphorylation may offer an explanation as to why the two phosphatases appear concurrently. When pH is higher, bp is active and when pH is lower, pap is active. In absence of pH adjustment, a second generation protein machine may require both enzymes in the system.

The free amino groups of lysine, histidine, and arginine residues on casein were the

potential interaction sites for DVS on casein. Intermolecular cross-linking occurred when the other side of DVS reacted with another free amino group on another chain although intramolecular cross-linking cannot be discounted [7]. Intramolecular cross-linking appeared to be minimal because robust materials were obtained that were capable of being hydrated without dissolving. We studied the kinetics of DVS interaction with casein in the pH range of 7-11[4]. The effective rate constant of the reaction (when using the same concentration of protein and same reaction time) increased with pH. This was from increased amounts of deprotonated amines. We have found that deprotonated amino acids were essential for casein to cross-link with DVS because we were unable to cross-link proteins without an abundance of them. We also identified the optimal pH range for the cross-linking reaction on casein at pH 10-11. This meant that, like in other reactions of amine addition to the electrophilic ethylene bond [8–10], the deprotonated amino group was nucleophilic. The reaction was fast because varying the reaction time 6, 12, and 24 hours did not produce any differences in the resulting protein gel.



### Polymeric acid protein behavior

Figure 3.5 Polymeric acid behavior: (a) dry protein; (b) hydrated protein at pH 7; (c) hydrated protein at pH 13; and (d) hydrated protein at pH 3

A simple model of the chemical structure of the cross-linked casein-based protein machine is shown in Figure 3.5 and depicts how it behaved as a polymeric acid. DVS served as a linkage to bond two protein chains together to make the insoluble but highly hydrated protein gel. When hydrated, the protein was an elastic rubber. The presence of negatively charged phosphate side groups repelled each other and expanded the network as shown in Figure 3.5 (b). In Figure 3.5 (c) the network expanded to its maximum volume at high pH ( $\text{pH} \gg \text{pK}_a^{2-}$ ) because of maximum ionization. At low pH, i.e.,  $\text{pH} \sim \text{pK}_a^-$ , the nearly uncharged phosphate caused complete contraction and loss of water as shown in Figure 3.5 (d).

Figure 3.6 shows how the protein machine contracts at constant pH using phosphatase. The loss of the negative charge contracts the protein gel with a concurrent loss of some but not all water (not as much as in Figure 3.5 (d)).

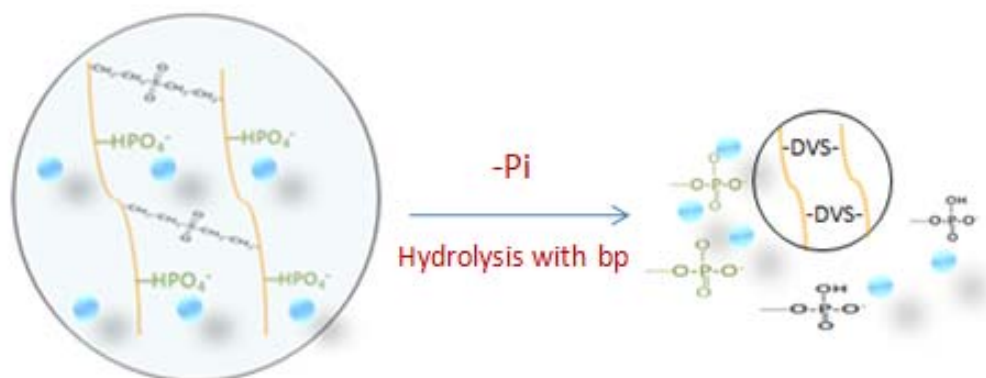


Figure 3.6 Proposed model of dephosphorylation process with bp at neutral pH

### 3.5 Conclusions

We have synthesized a protein gel that behaved as a typical polymeric acid able to expand at high pH and contract at low pH. The unique feature of our system was the ability to contract at constant pH by removing negatively charged phosphate groups with bovine phosphatase. Bovine phosphatase was found to be the more relevant phosphatase enzyme at physiological conditions. In absence of pH adjustment, it was found that the majority of gel volume contraction was from loss of negatively charged phosphate groups.

### 3.6 References:

1. Kim A. Deal, Judith N. Burstyn, Mechanistic Studies of Dichloro(1,4,7-triazacyclononane)copper(II)-Catalyzed Phosphate Diester Hydrolysis. *Inorg. Chem*, 35, 2792-2798, 1996
2. Bingham, E. W., Farrell, H. M., Jr., & Dahl, K. J, Removal of phosphate groups from casein with potato acid phosphatase. *Biochimica et Biophysica Acta*, 429(2), 448-460, 1976
3. Jean. L. Courthaudon, Bernard Colas, Denis Lorient. Covalent Binding of Glycosyl Residues to Bovine Casein: Effects on Solubility and Viscosity. *J. Agric. Food Chem*, 37, 32-364, 1989
4. Sereikaite I, Bassus D, Bobnis R, Denis G, Bumialene Zh, Bumialis BA, Divinyl sulfone as a cross-linking reagent for oligomeric proteins. *J Dairy Sci*, 78: p. 36-43, 1995
5. Xabier L, M. Schaefer, A. Dejaegere, M. Karplus. Theoretical Evaluation of pKa in Phosphoranes: Implications for Phosphate Ester Hydrolysis. *Journal of the American Chemical Society*, 124 (18), 5010-5018 , 2002
6. Silva, G., E.M. Kennedy, and B.Z. Dlugogorski, Effect of added nucleophilic species on the rate of primary amino acid nitrosation. *Journal of the American Chemical Society*, 127(11): p. 3664-3665, 2005
7. Sereikaite, J.; Bassus, D.; Bobnis, R.; Dienys, G.; Bumeliene, Z.; Bumelis, V.-A., Divinyl sulfone as a crosslinking reagent for oligomeric proteins. *Russian Journal of Bioorganic Chemistry*, 29, (3), p. 227-230, 2003
8. Berna, P.P, Porath, J., *J. Chromatogr*, vol. 753, pp. 57-62, 1996
9. Kurokawa, N. and Y. Ohfuné, Synthetic Studies on Antifungal Cyclic-Peptides, Echinocandins - Stereoselective Total Synthesis of Echinocandin-D Via a Novel Peptide Coupling. *Tetrahedron*, 49(28): p. 6195-6222, 1993
10. Nagy, I.B., et al., Conjugation of HS-oligopeptides with polymeric branched chain polypeptides containing multiple amino groups. *Journal of Bioactive and Compatible Polymers*, 15(2): p. 139-154, 2000

## CHAPTER 4

# Demonstration of full cycle and thermodynamic analysis of the protein machine

### 4.1 Abstract

In this chapter, dephosphorylated casein gel (described in Chapter 3) was re-phosphorylated using standard casein kinase activity protocols and the presence of  $P_i$  on the protein was determined using spectroscopy. Fourier transform-infrared (FT-IR) spectroscopy and physical volume changes proved the re-phosphorylation reaction in the presence of casein kinase, enzyme cofactor, and ATP. The re-attachment of negatively charged  $P_i$  on the protein re-expanded the network though not back to its original volume. A simple thermodynamic analysis was made to determine the work obtained from the protein machine. A significant positive heat evolution,  $\Delta Q$ , will detract from obtainable work and appeared as an enthalpic term in the free energy analysis.

### 4.2 Introduction

Biochemical reaction systems in living cells are open. This means they exchange materials with their environment and utilize chemical energy, usually in the form of adenosine triphosphate (ATP) hydrolysis, with concurrent dissipation of heat. Technically, no matter how complex a biochemical reaction system is, if it is left alone in a closed system, it will gradually decay and die. In terms of physical chemistry, a closed system has no life [1]. This is true for all living systems, even those as simple as a single motor protein [2, 3].

Casein protein contains the peptide sequence serine (S) or threonine (T) bonded to any amino acid (X), which in turn is bonded to an acidic amino acid such as glutamic or aspartic acid or an already phosphorylated serine or threonine (Acid), {S/T-X-Acid} [4]. Some of the serine or threonine hydroxyl end groups are phosphorylated in natural whole casein. Normally,  $\alpha$ -casein has 8 phosphate groups in 199 amino acids while there are 5 phosphate groups of 209 amino acids in  $\beta$ -casein [5]. The phosphate groups can be



cleaved by phosphatase as we introduced in Chapter 3 and then be re-phosphorylated at the S/T positions by casein kinase and ATP. Kinase is an enzyme capable of hydrolyzing ATP and placing the phosphate ion onto the hydroxyl. The phosphate ion is  $2^-$  at current near physiological conditions. We have developed a casein gel with the potential to expand or contract with changes in pH, ionic strength, or by addition/removal of phosphate ions. When hydrated at constant  $\text{pH} > \text{pK}_a$ , the negatively charged phosphate ions repel each other and expand the network. When dephosphorylated, the network contracts and loses some, but not nearly all, water.

The objective of this chapter is to

1. Demonstrate the apparently more complex expansion cycle.
2. Estimate the protein machine work,  $\Delta G$ , and efficiency,  $\eta$ , and compare them to actual protein motors.

## 4.3 Materials and methods

### 4.3.1 Materials

Bovine phosphatase (20 mg protein/ml, 6202 units/mg protein, liquid), casein, casein kinase (59 units/ml, liquid), adenosine-5'-triphosphate (ATP, 99+ %, powder), manganese chloride ( $\text{MnCl}_2$ , 99+ %, powder), and divinyl sulfone (DVS, 97% with 0.05% hydroquinone, liquid) were obtained from Sigma-Aldrich and were used without further modification.

### 4.3.2 Preparation of protein machine

The protein machine, in the form of a DVS cross-linked casein gel, was prepared as per the protocol in Chapter 3.

### 4.3.3 Preparation of re-phosphorylated casein rubber

Casein had 8 {S/T-X-Acid} sequences [5]. It was proposed to run phosphorylation reactions on already dephosphorylated casein gel using standard casein kinase activity protocols. The dephosphorylated casein gel was described in Chapter 3. Therefore, a full

cycle could be demonstrated on the same protein gel. We utilized the casein phosphorylation protocol of Bingham [6]. With the help of ATP, casein kinase could re-phosphorylate the dephosphorylated casein at the optimum condition of pH 7.6. In order to maximize its activity, casein kinase needs the presence of a divalent cation. In our experiment, we chose  $Mn^{2+}$  in the form of manganese chloride. The activity of casein kinase was assessed on uncross-linked but dephosphorylated casein (casein kinase substrate) in the presence of ATP alone and ATP and  $MnCl_2$  cofactor by measuring the UV-Visible absorbance at 410 nm.

Based on the experiment of Chapter 3, Part 3.3.5, we first hydrated as-molded, dry cross-linked casein samples in 300 ml pure DI water for two hours. At pH 9 the gel was dephosphorylated by adding 5  $\mu$ l bp into the solution and stirring. At 60 h, 8  $\mu$ l casein kinase, 0.1 mg  $MnCl_2$ /ml solution, and 0.55 mg ATP/ml solution was added. The volume change and pH were monitored as a function of time. Figure 4.1 illustrates the step-by-step procedure to make the re-phosphorylated gel.

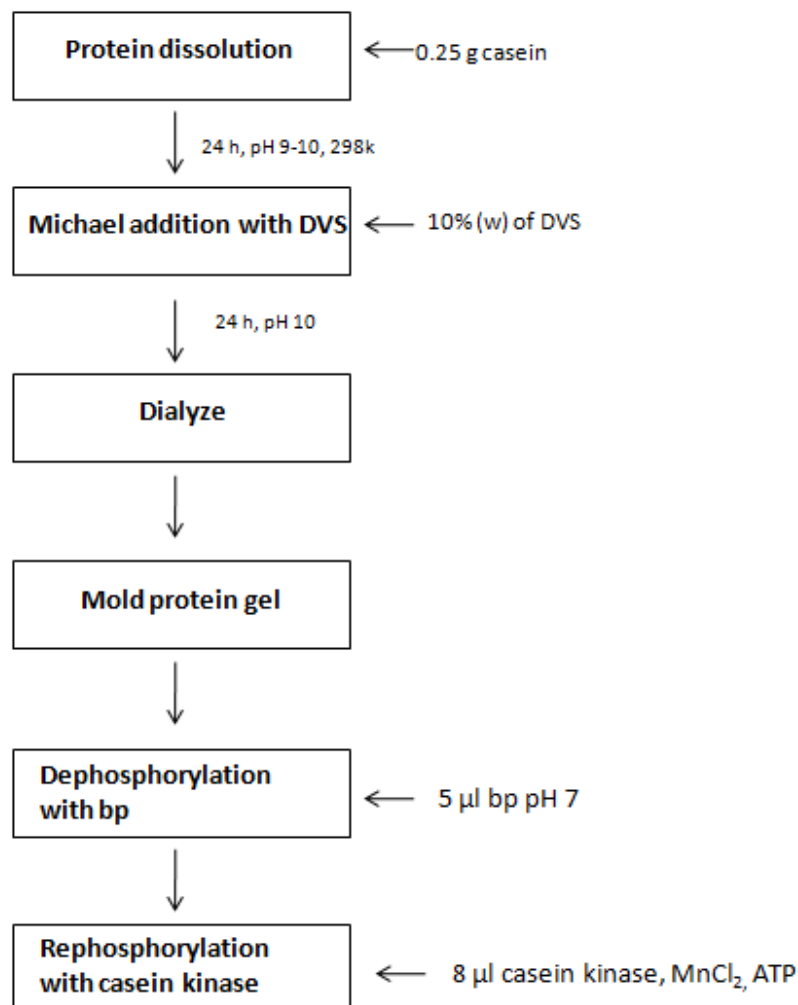


Figure 4.1 Experimental protocol to demonstrate one cycle of the protein machine

#### 4.3.4 Fourier transform-infrared (FT-IR) spectroscopy

FT-IR analysis was performed with a Thermo Nicolet 6700 with a diamond attenuated total reflectance (ATR) crystal. Pressure was applied to each sample to ensure good sample/crystal contact. A resolution of  $4\text{ cm}^{-1}$  was used over 64 scans. Background spectra were obtained before each analysis with blanks run between samples to ensure that there was no crystal contamination. Prior to examination, samples were dialyzed using the same procedure employed after cross-linking then dried under vacuum.

## 4.4 Results

### 4.4.1 Phosphorylation of casein kinase substrate

Figure 4.2 shows that dephosphorylated casein could only be re-phosphorylated with casein kinase and ATP using a divalent metal cation cofactor as has been observed previously [7].

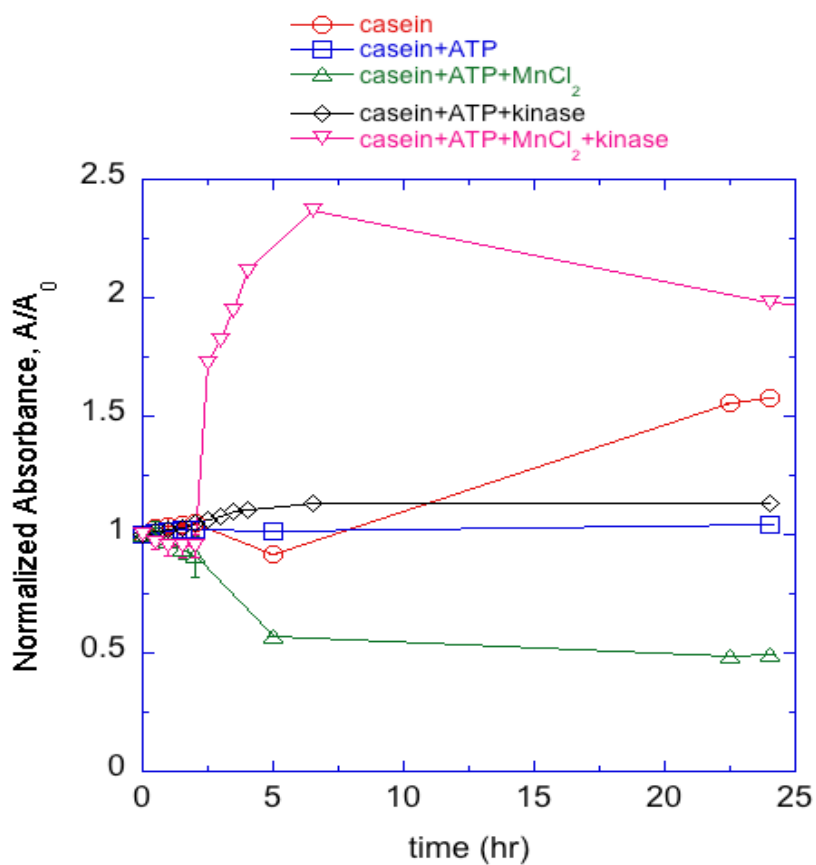


Figure 4.2 Normalized UV-Visible absorbance of casein phosphorylation reaction

### 4.4.2 Demonstration of one full protein machine cycle

Cross-linked casein gel was dephosphorylated by bp at pH 9. Release of phosphate ions reduced the pH of the solution from 9 to 7 within the first 48 hours and the

dephosphorylated protein contracted to ~20% of its original volume. At 60 h, casein kinase,  $Mn^{2+}$ , and ATP were added to the solution. 60 h was determined to be a sufficient time at pH 7-9 to fully de-phosphorylate the protein as observed in Figure 3.4. The pH immediately dropped from release of  $P_i$  and protons as ATP was hydrolyzed. We adjusted the pH back to 7 to allow the re-phosphorylation reaction to run. The volume and pH change is shown in Figure 4.3. A lag time was observed before the casein gel began to re-expand. At long time, the casein gel was not able to return to its original volume, attaining a final value of 40% of its original volume before the gel began to deteriorate, which was the reason for the increased error in volume measurements in this time region. Besides deterioration of the casein gel, other factors may have influenced the inability of the gel to regain its volume in a sufficient time. One was the  $Mn^{2+}$  cofactor, which could screen negative charge on  $P_i$ . The other was potential aggregation of the casein molecules after experiencing a low pH, which will be explored next.

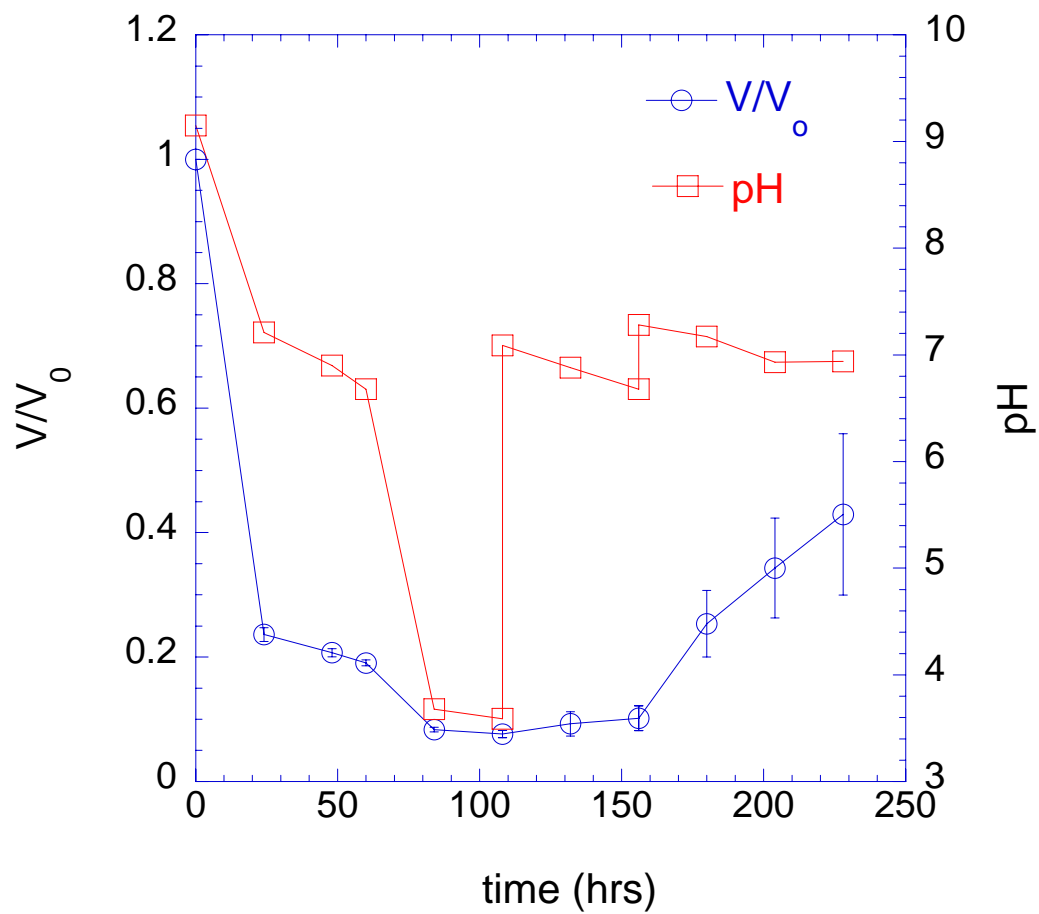


Figure 4.3 Dephosphorylation and re-phosphorylation cycle of casein gel. Average volume change is blue line and average pH is red line

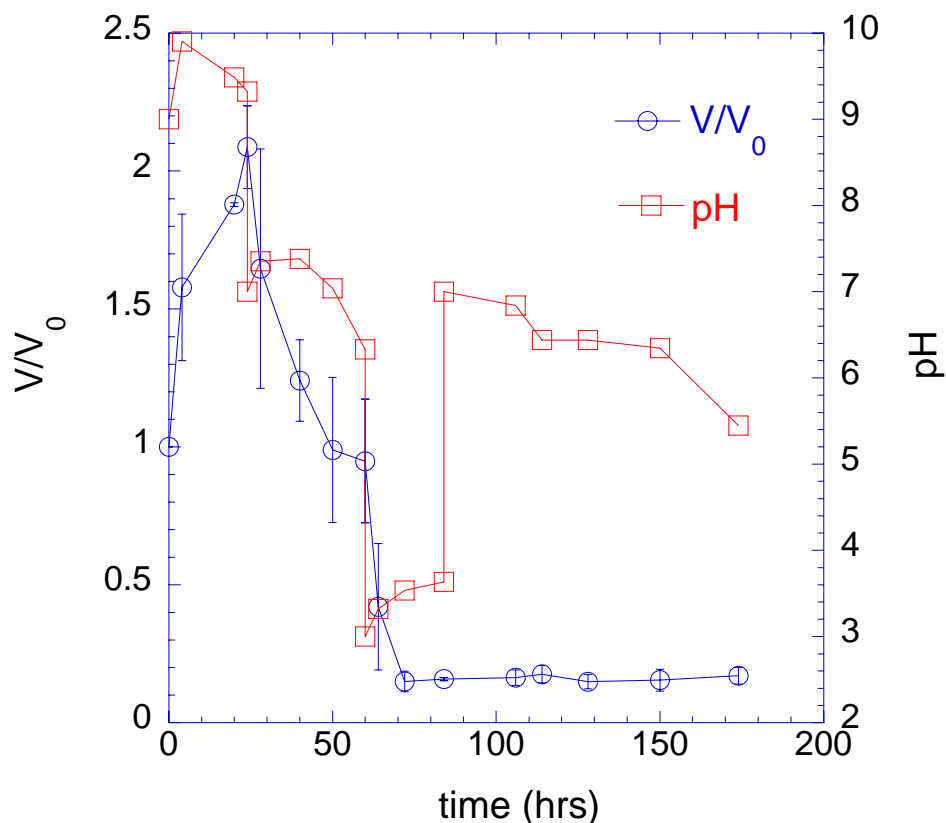


Figure 4.4 Casein gel volume change in water with the same pH adjustment as in Figure 4.3

In order to assess the influence of pH on volume change, we performed another experiment in pure DI water without any enzymes. The pH was manually adjusted to mimic the pH changes occurring in Figure 4.3. First, the gel was hydrated in water for 2 hours, and then the pH was adjusted to 9, and adjusted again to pH 7 at 24 h. At 60 h, pH was decreased to 3 and increased back to pH 7 at 84 h. At low time, the casein gel responded as expected to the change in pH as per its polymeric acid characteristic. However, the casein gel did not re-hydrate and re-expand at long times at pH 7.

#### 4.4.3 Fourier transform-infrared (FT-IR) spectroscopy

FT-IR spectroscopy can monitor the dephosphorylation and re-phosphorylation reactions on the casein gel via changes in the Amide I peak at  $\sim 1630 \text{ cm}^{-1}$ . The exact band position was determined by the backbone conformation and the hydrogen-bonding

pattern between peptide bond carbonyls on one protein molecule and peptide bond amines on another protein molecule [7]. Figure 4.5 shows that the re-phosphorylated gel returns to its original Amide I position after a very large shift to lower wavenumber, indicating that a more native conformation returned. The samples were taken from the experiment depicted in Figure 4.3 at time=0 h (red, native phosphorylated casein gel), 72 h (blue, dephosphorylated casein gel), and 228 h (green, re-phosphorylated casein gel).

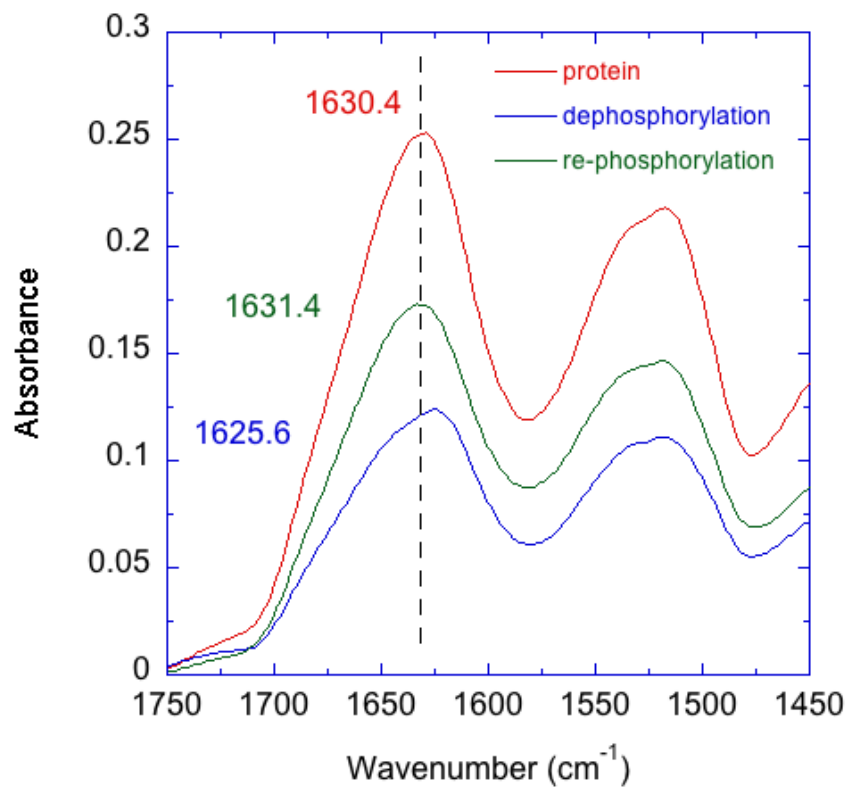


Figure 4.5 FT-IR spectra showed Amide I shift. Red: native casein cross-linked with DVS; blue: same sample dephosphorylated; green: same sample re-phosphorylated



The dephosphorylation and re-phosphorylation reactions also showed changes in the FT-IR spectrum in the fingerprint region. From Figure 4.6 we can conclude several results. First, S=O absorbances at 1237 and 1119  $\text{cm}^{-1}$  appeared, which were absent in native casein but present in the cross-linked gel and indicated that DVS was present. Second, re-phosphorylation returned a significant absorbance from C-O-P at around 1000  $\text{cm}^{-1}$ , which was the phosphate attached to a protein carbon [7-10].

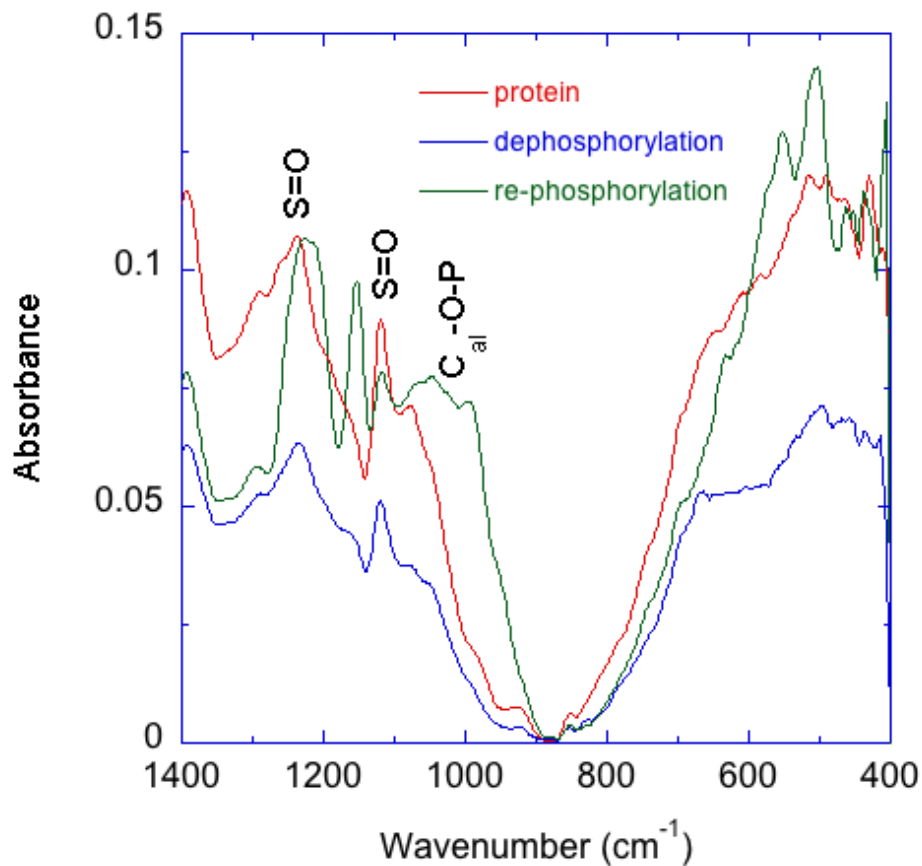


Figure 4.6 FT-IR spectra demonstrated dephosphorylation and re-phosphorylation reactions

The very broad shoulder between 1100 and 990  $\text{cm}^{-1}$  was primarily assigned to the asymmetric stretching vibration of C-O-P groups. But it has been shown that  $\nu_{\text{as}}(\text{O-P-O})$  and  $\nu_{\text{s}}(\text{O-P-O})$  could have contributed [11-14]. Previous spectroscopic studies [14] reported the asymmetric stretching vibration of the metaphosphate group,  $\nu_{\text{as}}(\text{PO}_3)$ , in the range 1080–1120  $\text{cm}^{-1}$ . Therefore, in the FT-IR spectra presented, there could be

contributions from phosphate itself in the 1100-990  $\text{cm}^{-1}$  shoulder. However, the samples were dialyzed prior to analysis so these most likely originated in bound phosphate and not free phosphate. The broadening of the 1200-1250  $\text{cm}^{-1}$  peak in the re-phosphorylated gel also originated in re-attached phosphate because the original gel had this broad peak and the dephosphorylated gel did not.

A new peak in the re-phosphorylated casein gel appeared at 1170  $\text{cm}^{-1}$  that did not originate in phosphate. This peak was from a new state of hydroxyl containing amino acids, where phosphorylation took place. Although the Amide I suggested that a more native polymer conformation returned, the state of individual amino acids, especially ones involved in phosphorylation, was not achieved.

FT-IR analysis did not offer insight into why the gel in the pH adjustment experiment did not re-expand. de Kruif & Zhulina have reported that acid-induced flocculation of casein micelles and presumably also casein nanogel particles, is a result of a collapse of the  $\kappa$ -casein brush because of reduced solvency due to reduced dissociation of glutamic acid residues in the C-terminus of  $\kappa$ -casein [15]. It was possible that the natural structure of casein caused it to aggregate. Without an external stimulus to break up the aggregated casein, like the phosphorylation reaction, the casein remained aggregated.

To explain the associative properties of casein micelles, the molecular architecture hierarchies should be carefully studied. Casein micelles, which consisted of 94% protein and 6% inorganic materials, had a radius of 100 nm [15]. In each micelle, there were around 900 structural elements called nanoclusters [16]. Nanoclusters are comprised of a core of amorphous calcium phosphate surrounded by a shell of  $\alpha_{s1}$ -,  $\alpha_{s2}$ - and  $\beta$ -caseins whose centers of phosphorylation participate in the core via ionic interactions [17]. Several factors were likely to contribute to the force to integrate nanoclusters to form casein micelles, for example, cross-linking of nanoclusters by caseins containing multiple centers of phosphorylation and weak protein-protein interactions, including hydrophobic and electrostatic interactions and hydrogen bonding [15, 18]. There is ample evidence and consensus that the casein micelle is sterically stabilized by a traditionally termed “hairy layer” of  $\kappa$ -casein molecules [16, 19]. At the periphery of the particles is the glycomacropeptide (GMP) portion. As GMP carries 14 carboxylic acid groups, it can be

considered a salted polyelectrolyte brush. An extended brush provides the required steric stabilization. The properties of the micelles can be described generally by adopting the adhesive hard sphere (AHS) model of Holt [19] illustrated in Figure 4.7.

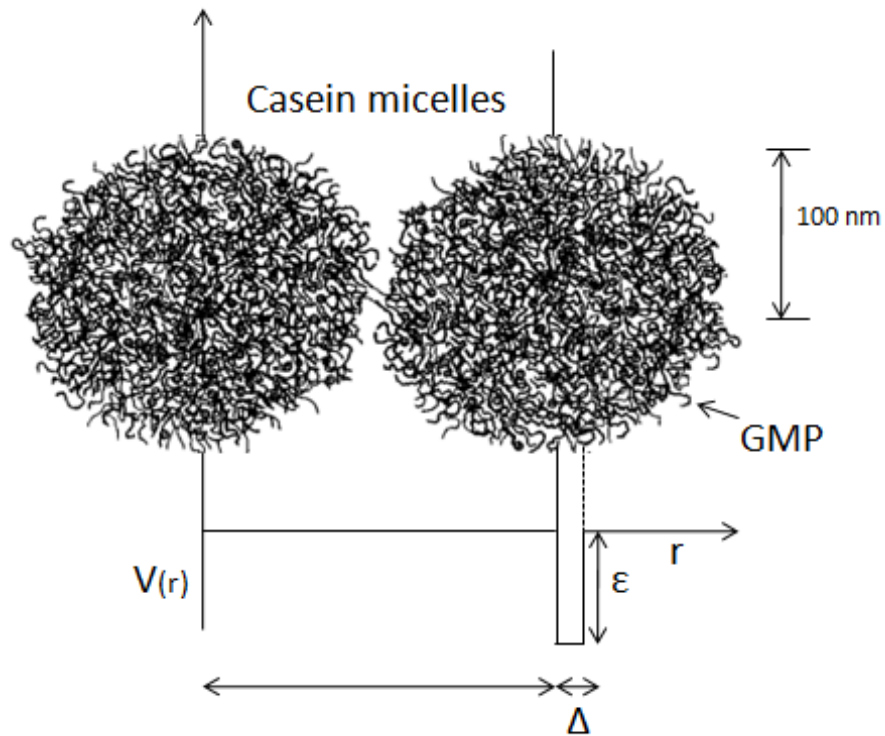


Figure 4.7 Schematic representation of casein micelle [19]. Polyelectrolyte "hairs" provide steric stabilization. The interaction between the hairs is modeled as a square-well adhesion of depth  $\epsilon$  and width  $\Delta$

When two particles meet, the steric stabilization coming from the polyelectrolyte-type protein will keep the particle in a relatively constant position as the repulsive force between two micelles increases significantly on contact. The repulsive force coming from GMP depends on the anchoring density, chain length, charge density and ionic strength. In our experiment, casein was well hydrated at high pH because of increased charge density and ionic strength of GMP. These groups make the chain hydrophilic. It is possible to envision that the repulsive GMP is somehow damaged by acid and the casein micelle particles will experience attractive Van de Waals interactions. The deficit of secondary and tertiary protein structure meant casein brushes collapsed at low pH and steric stabilization was absent so strong attractions and cross-linking made the system

solidify. For instance, the acid-induced flocculation of casein is routinely utilized in yogurt making. Lactic acid bacteria convert lactose into lactic acid and reduce pH to cause casein flocculation.

Secondary effects from possible casein flocculation aside, a simple model is used to summarize the physics of the protein machine as shown in Figure 4.8. A cross-linked phosphoprotein, casein, could be dephosphorylated and re-phosphorylated. In its original phosphorylated state at near physiological conditions, the phosphate ions were  $\text{PO}_3^{2-}$  and 9 negative charges per chain were able to repel each other and greatly expand the network when fully hydrated. Dephosphorylation by bovine phosphatase caused the casein gel to contract. The casein gel was re-expanded by re-phosphorylating the protein with ATP using casein kinase. The re-phosphorylated protein did not return to its original state for 2 possible reasons: the kinase  $\text{Mn}^{2+}$  cofactor interfered with expansion by screening negative charge and/or the low pH damaged the protein by causing flocculation.

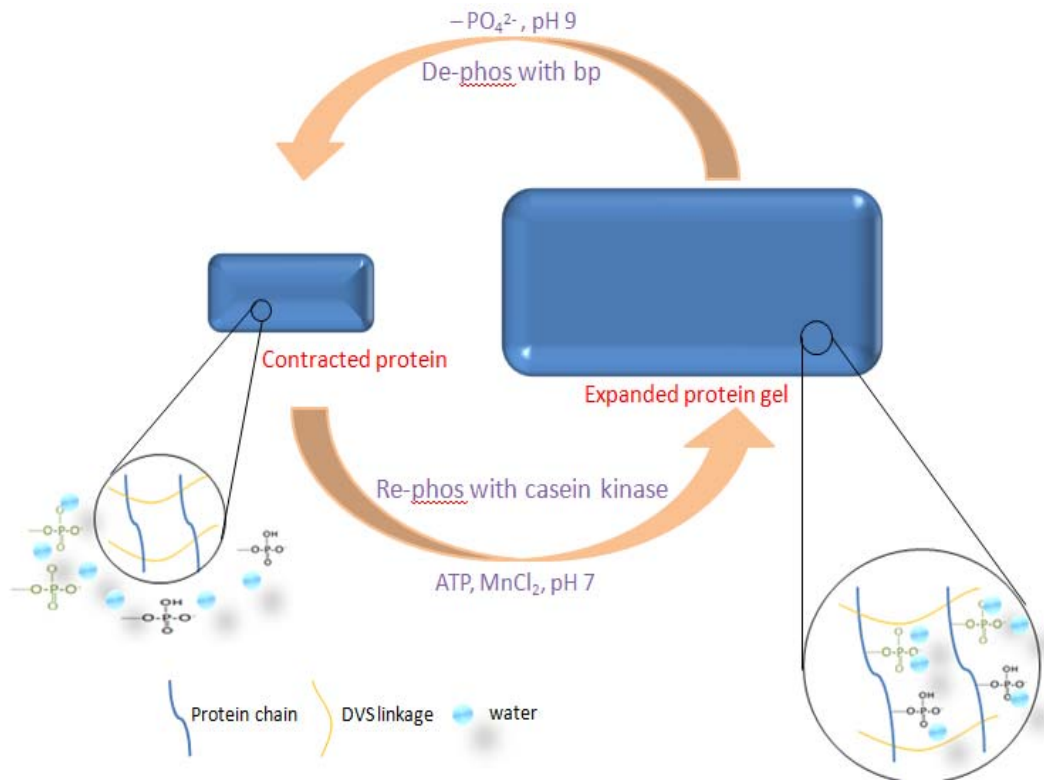


Figure 4.8 Illustration of protein machine expansion and contraction cycle

## 4.5 Thermodynamic Analysis of the Protein Machine

Upon hydration, the dry protein rubber will expand to a state similar to that in Figure 3.5 (a). Water occupies free volume and swells the protein rubber so there is a loss of entropy as the protein molecules are stretched. Water also solvates the protein molecules, which is a positive contribution to entropy. So there is an entropy competition between solvation, which encourages the chains to move freely and attain any conformation, and stretching, which forces them into a non-natural, straight conformation. Water hydrogen bonds to the protein and proteins hydrogen bond to themselves and other protein molecules. The hydrogen bonding produces heat (a heat of mixing) that contributes to enthalpy.

When attached to the protein,  $P_i$  has a low entropy but free  $P_i$  has a high entropy because it can diffuse anywhere in the solution. Water is also lost and gained during the contraction/expansion process as shown in Figure 3.5 so there is a contribution to entropy from water content.

Protein molecule chain extension/contraction is purely entropic and can be described by classical rubber elasticity theory [20] to produce an elastic contribution to free energy,  $\Delta G_{el}$ .

Diffusion of  $P_i$  and water is also purely entropic and can be described by a concentration gradient to produce a transport component of free energy,  $\Delta G_t$ .

Solvation is entropic and enthalpic. The entropic portion can be described through simplifications of statistical thermodynamics such as Flory-Huggins theory. However, the enthalpic contribution has no easy treatment especially if it is significant. Combined, they produce a mixing contribution to the free energy,  $G_{mix}$ . Therefore, the total free energy of the protein machine is

$$\Delta G_T = \Delta G_{el} + \Delta G_t + \Delta G_{mix} \quad (1)$$

The gain/loss of  $P_i$ , the expansion/contraction of the network, and the gain/loss of  $H_2O$  are reversible processes and controlled by the enzymes,  $P_i/ATP$  concentration, and the elasticity of the network. At equilibrium ( $G_T=0$ ), the protein machine can be described by experimentally determined parameters:

$$\int Fdx = \int PdV = T\Delta S - \Delta Q . \quad (2)$$

The first term is the area under a force-displacement curve and is experimentally determined by, for instance, re-phosphorylating the protein while contained between compression plates on a mechanical testing instrument. The second term is experimentally determined from the osmotic pressure of the gel and volume change, i.e., it is the same experiment as the force-displacement experiment.  $\Delta Q$  is the heat of mixing and is experimentally determined from calorimetry.

Comparing muscle to our protein machine, it is assumed that the thermodynamics of the biochemical reactions between the two are similar given that both systems operate on similar enzymatic reactions utilizing ATP. Differences arise in the mechanism by which each moves as a result of those reactions. Both have protein conformational changes. However, the movement of muscle means that the original state is never regained so there is loss when the protein attains a new conformational state. The largest loss is heat from sliding friction between the actin and myosin. In our system, the protein molecules have the potential to regain their original conformation if flocculation and charge screening can be eliminated. The largest loss is from a heat of mixing between water and protein and protein and another protein.

According to M. Rubinstein and R.H. Colby equation, we can very simply estimate an elastic contribution to the free energy and the approximate results are shown in below equation [22]:

$$\Delta G_{el} \approx RT \left(\frac{V}{V_0}\right)^{\frac{2}{3}} \quad (3)$$

Where V is casein swollen gel volume and  $V_0$  is the original dry gel volume, R is the gas constant, and T is absolute temperature. The unit of  $\Delta G_{el}$  is J/mol and we term this function as “R+C” for simplicity. L.R.G. Treloar also defined the free energy of swollen rubber in an approximate equation with a unit of J/mol [21]:

$$\Delta G_{el} \approx \frac{1}{2} RT \left[ 3 \left(\frac{V}{V_0}\right)^{\frac{2}{3}} - 3 \right] \quad (4)$$

Originally, Treloar deduced function (4) from an accurate expression based on classical rubber elasticity theory:

$$\Delta G_{el}' = \frac{1}{2}NKTv_2^{\frac{1}{3}}\left[3\left(\frac{V}{V_0}\right)^{\frac{2}{3}} - 3\right] \quad (5)$$

N is the chains number per unit volume of the gel network; K is Boltzman constant;  $v_2$  refers to volume fraction of polymer in the mixture of polymer and liquid. In this equation,  $\Delta G_{el}$  has a unit of  $J/m^3$ . Function (5) could be approximately converted into (4) by timing the molecular volume so the former could be calculated readily. We denote equation (4) and (5) into “Treloar a” and “Treloar b” separately. Therefore, it’s reasonable for us to estimate the elastic free energy ranges of  $\Delta G_{el}$  in our protein machine system according to functions (3), (4) and (5) as shown in Fig 4.9:

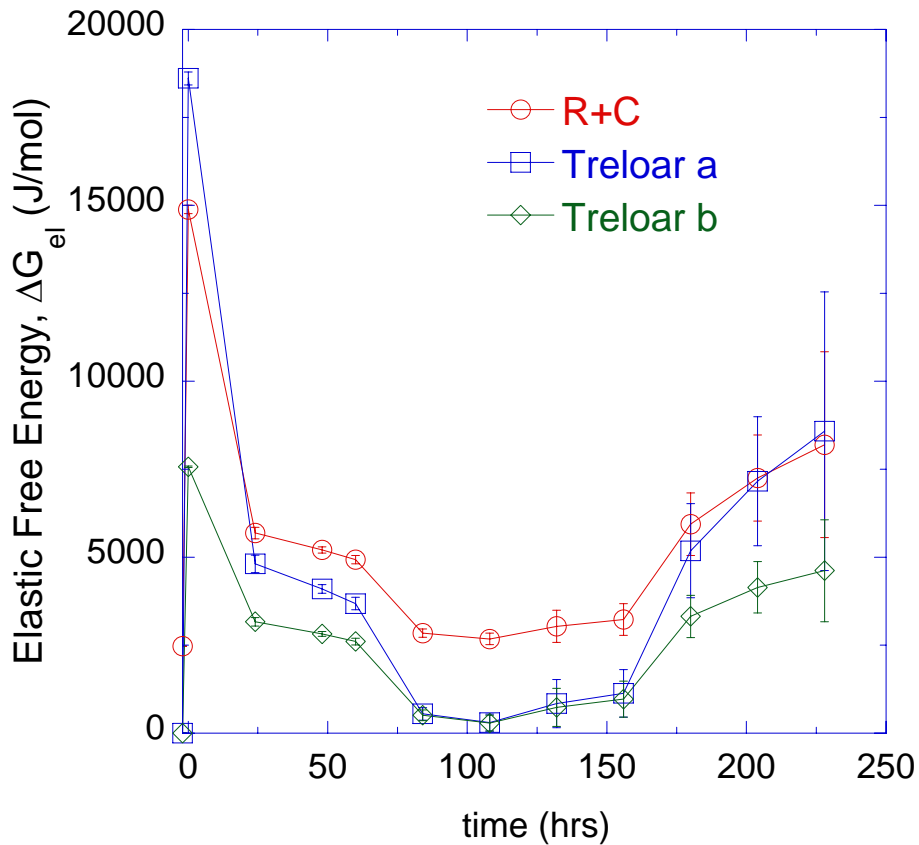


Figure 4.9 Estimation of elastic contribution to free energy

Within experimental error, the casein gel proved to be “resilient” or able to recover its original molecular conformation through a contraction and expansion cycle. Considering that the free energy of ATP hydrolysis is  $\Delta G_0=30.5$  kJ/mol, the elastic component of the free energy yields a maximum efficiency range of  $\eta=\Delta G_{el}/\Delta G_0\sim 15\text{-}30\%$  which is a promising start show in Fig 4.10 [11]. Future work will focus on a more exact experimental determination of  $\Delta G_T$  because other contributions will factor in significantly.

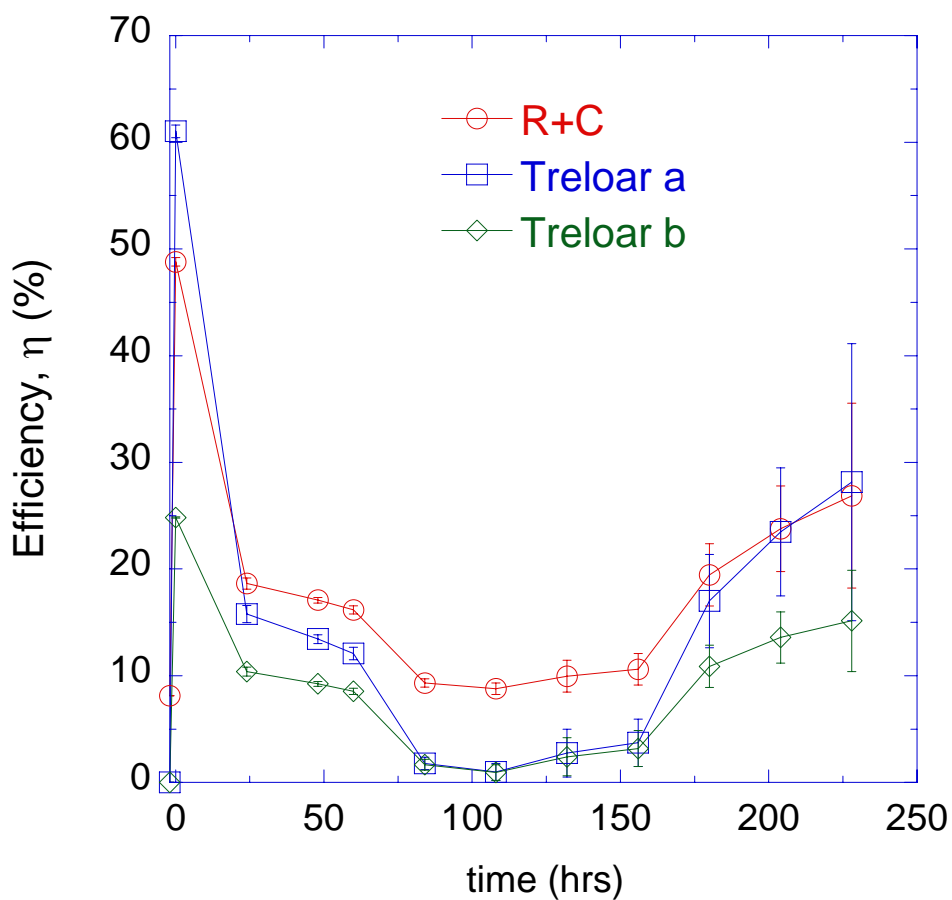


Figure 4.10 Estimation of elastic free energy efficiency



## 4.6 Conclusion

Using an already dephosphorylated casein gel, we have re-phosphorylated the gel using casein kinase and ATP at neutral pH. Fourier transform-infrared (FT-IR) spectroscopy was employed to detect the various states of  $P_i$  on the protein through dephosphorylation and re-phosphorylation. Just like the original cross-linked protein gel, the recombination of the phosphate groups could allow the gel to expand again. At long time, the casein gel was not able to return to its original volume, attaining a final value of 40% of its original volume before the gel began to disintegrate. In this chemical energy conversion process, nothing is needed to put into the biological systems except enzyme, enzyme cofactor and ATP and the FT-IR spectroscopy and gel volume changes demonstrated the process. The mechanical work derived from the protein motor can be determined by a simple thermodynamic analysis. The elastic component of the free energy yields an efficiency return of  $\sim 30\%$ , which is a promising start. A challenge going forward will be determining the other components of the total free energy  $\Delta G_T$ .

## 4.7 References:

1. Nicolis G, Prigogine I. *Self-Organization in Nonequilibrium Systems*. New York: Wiley-Interscience, 491 pp.2, 1997
2. Qian H. The mathematical theory of molecular motor movement and chemomechanical energy transduction. *J. Math. Chem*, 2000, 27:219–343
3. Qian H. Cycle kinetics, steady-state thermodynamics and motors: a paradigm for living matter physics. *J. Phys. Cond. Matt*, 17:S3783–944, 2005
4. Gu, S., G. H. He, et al. Preparation and characteristics of crosslinked sulfonated poly (phthalazinone ether sulfone ketone) with poly(vinyl alcohol) for proton exchange membrane. *Journal of Membrane Science* 312(1-2): 48-58, 2008
5. Masaaki Yoshikawa, Ryuzo S, Hideo C, A rapid and sensitive assay method for protein kinase. *Agricultural and Biological Chemistry*, Vol.45, No.4, pp. 909-914, 1981
6. Li, K., *Synthesis of lignin-carbohydrate model compounds and neolignans*, in Department of Wood science and forestry products, Virginia Polytechnic Institute and State University: Blacksburg, VA, 1996
7. Bingham, E. W., Farrell, H. M., Jr., & Dahl, K. J, Removal of phosphate groups from casein with potato acid phosphatase. *Biochimica et Biophysica Acta*, 429(2), 448–460, 1976
8. M. Jackson, H. H. Mantsch, *The Use and Misuse of FTIR Spectroscopy in the Determination of Protein Structure*, *Critical Reviews in Biochemistry and Molecular Biology*, 30(2):95-120, 1995
9. Mehdipour-Ataei, S., M. Hatami, et al. Organosoluble, Thermally Stable Polyamides Containing Sulfone and Sulfide Units. *Chinese J. of Polymer Science*, 27(6): 781-787, 2009
10. Malonga, H., J. F. Neault,. DNA interaction with human serum albumin studied by affinity capillary electrophoresis and FTIR spectroscopy. *DNA & Cell Biology* 25(1): 63-68, 2006
11. Liu, M., M. Krasteva,. Interactions of phosphate groups of ATP and aspartyl phosphate with the sarcoplasmic reticulum Ca<sup>2+</sup>-ATPase: An FTIR study. *Biophysical Journal*, 89(6): 4352-4363, 2005
12. Nathan Yee, Liane G. Benning, Vernon R. Phoenix, F. Grant Ferris, *Characterization of Metal-Cyanobacteria Sorption Reactions: A Combined Macroscopic and Infrared Spectroscopic Investigation*. *Environ. Sci. Technol*, 38, 775-782, 2004
13. F. Ronzon et al. Behavior of a GPI-anchored protein in phospholipid monolayers at the air-water interface. *Biochimica et Biophysica Acta*, 1560, 1-13, 2002
14. T. Theophanides., *Fourier Transform Infrared Spectra of Calf Thymus DNA and its Reactions with the Anticancer Drug Cisplatin*, *Applied Spectroscopy*, Volume 35, Number 5, 1981
15. Bayden R. Wood, Brian Tait, Donald McNaughton, *Fourier-Transform Infrared Spectroscopy as a Tool for Detecting Early Lymphocyte Activation:A New Approach to Histocompatibility Matching*, *Human Immunology* 61, 1307–1315, 2000

16. C.G. de Kruif, Ekatherina B. Zhulina,  $\kappa$ -casein as a polyelectrolyte brush on the surface of casein micelles, *Colloids and Surfaces A: Physicochemical and Engineering Aspects*, 117,151-159, 1996
17. Holt, C., D. Horne, The hairy casein micelle: evolution of the concept and its implications for dairy technology. *Neth. Milk Dairy J.* 50:85–111, 1996
18. C. G. de Kruif, Supra-aggregates of Casein Micelles as a Prelude to Coagulation, *J Dairy Sci* 81:3019–3028, 1998
19. Holt, C., Structure and stability of the bovine casein micelle. *Advances in Protein Chemistry*, P. 63–151 Acad. Press, New York, NY, 1992
20. Holt, C, The biological function of casein? P. 60–69 in *HRI Year book for 1994*. Hannah Res. Inst., Ayr, Scotland, 1995
21. L. R.G. Treloar. *The physics of rubber elasticity*. Oxford University Press, Oxford, Pp. 59-70, 2005
22. M. Rubinstein and R.H. Colby, *Polymer Physics*. Oxford University Press, Oxford, Pp. 274-275, 2003

## CHAPTER 5

### Conclusion

Nature can readily convert chemical energy into mechanical work at mild conditions of pH 7, 37°C, physiological ionic strength, and standard pressure. The muscle sliding filament system, made of myosin and actin, takes advantage of the "energy-rich" pyrophosphate bond in ATP to allow the thin actin filament to slide over the thick myosin filament. The sliding mechanism produces a huge frictional loss that is used by the body for heat but would be too much for an engineering purpose. In an attempt to lower or eliminate losses, especially from sliding friction, we proposed a protein gel that behaves like a polymeric acid able to respond to pH or ionic strength change but instead undergoes phosphorylation and dephosphorylation reactions to initiate volume changes and therefore convert chemical energy to mechanical work.

In Chapter 3 we described the method to produce a cross-linked protein ionic gel by reacting divinyl sulfone (DVS) with nucleophilic amines on casein through the Michael addition reaction. The synthesis was conducted at pH 10, 298 K, physiological ionic strength, and 101 kPa eliminating the possibility of damaging the protein. Then we used bovine phosphatase (bp) to dephosphorylate the protein gel. Immediately, a pH drop was observed and the protein gel experienced a remarkable volume contraction. Results showed that the majority of the contraction came from dephosphorylation with screening of negative charge on the rest of the protein constituting a small portion. Fourier transform-infrared (FT-IR) spectroscopy and physical volume changes proved the cross-linking reaction and de-phosphoylation reaction in the presence of bp.

Chapter 4 centered on re-phosphorylation on the de-phosphorylated casein by casein kinase, enzyme cofactor, and ATP. The recombination of phosphate groups on the protein gel re-stretched the network at  $\text{pH} \geq \text{pK}_a^{2-}$ . FT-IR spectroscopy indicated that re-phosphorylated casein returned to its original Amide I position meaning a more native conformation regenerated. The de-phosphorylated casein showed a big shift to lower wavenumber. We also explored the work obtained from the protein machine and a simple thermodynamic analysis was constructed. A challenge going forward will be determining the various components of the total free energy  $\Delta G_T$ .

To summarize, this research provided several insights. We found optimal benign conditions to synthesize protein gels without damaging the native protein. We determined the dephosphorylation capacities of bovine phosphatase and potato phosphatase on protein gels. We developed a spectroscopic approach to monitor gel contraction and expansion cycles and concurrent biochemical reactions. We demonstrated direct conversion of chemical to mechanical energy at near physiological conditions. Finally, we offered a simple thermodynamic analysis to describe the whole process. The proposed protein gel could find possible applications in biomedical engineering like pH sensitive drug delivery or power vehicles, for direct tissue/muscle replacement, or to build an exoskeleton to enhance human performance.